Journal
of
The Franklin Institute
Devoted to Science and the Mechanic Arts

Vol. 231 JANUARY, 1941 No. 1

THE DETERMINATION OF AVERAGE MOLECULAR WEIGHTS OR PARTICLE SIZES FOR POLYDISPERSED SYSTEMS.

BY

ELMER O. KRAEMER,

Biochemical Research Foundation of The Franklin Institute.

With the exception of certain well-defined, crystallizable proteins and some synthetic products prepared under quite special conditions (3), macromolecular substances are commonly non-homogeneous in molecular weight. Fine powders and colloidally dispersed material are also typically polydispersed. The only generally applicable methods of determining the degree of heterogeneity of such materials without actually effecting a separation of the material into fractions depend upon sedimentation analysis. For the very finely divided dispersions and, particularly, for macromolecular substances, such analysis requires the application of the ultracentrifuge. Under the most favorable conditions, fractionation (e.g., by precipitation or solution methods) is relatively ineffective as well as laborious, and the results from the ultracentrifugal analysis of fractionated samples demonstrate that their degree of heterogeneity is quite pronounced (6, p. 353; 13, p. 437).

Owing to the highly specialized character of ultracentrifuge technic, the determination of an average molecular

(Note—The Franklin Institute is not responsible for the statements and opinions advanced by contributors in the JOURNAL.)

weight of a macromolecular substance is usually made by means of some physical or chemical property (e.g., osmotic pressure, viscosity, end-group, etc.) which is known or assumed to vary with molecular size or weight for the particular material in question. We have shown in previous publications (7, 8) that average molecular weights so obtained may differ, depending upon the relationship between the measured property and molecular size. In order, therefore, to compare results obtained for a given heterogeneous material by various methods, one must consider the types of average value which the different methods yield. A similar problem is encountered in the specification of the "average size" and size uniformity of fine powders, and has been discussed in considerable detail by investigators of cements, pigments, dusts, and such particulate material.

In the present paper we shall consider the interrelation between several types of average values of significance in the determination of both molecular weights and particle sizes by various indirect methods and shall determine the conditions under which different averages may be calculated from each other.

DEFINITIONS OF AVERAGE MOLECULAR WEIGHTS AND PARTICLE SIZES.

It has already been shown (8) that osmotic pressure, end-group determinations, ultramicroscopic counting (2) or any other method which depends in principle upon counting the molecules or particles in a sample of given weight yields what we chose to call a "number-average" molecular weight,[1] in line with the nomenclature introduced by Perrott and Kinney in connection with the specification of particle diameters (11). This average (M_n) is defined by the expressions

$$(1) \qquad M_n = \frac{\Sigma M_i n_i}{\Sigma n_i} = \frac{\Sigma w_i}{\Sigma w_i / M_i} = \frac{W}{N},$$

where n_i is the number and w_i is the weight of the molecules or particles having a weight M_i, and N is the total number of particles in W grams of sample.

[1] Molecular weight and particle weight are used synonymously in this paper.

Considering a continuous variation of molecular or particle weights, for which it is permissible to employ differential terminology,

$$(1a) \quad M_n = \frac{\int_0^\infty M \cdot f_n(M) \cdot dM}{\int_0^\infty f_n(M) \cdot dM} = \frac{\int_0^\infty f_w(M) \cdot dM}{\int_0^\infty \frac{1}{M} \cdot f_w(M) \cdot dM},$$

where $f_n(M)$ and $f_w(M)$ are the functions describing, respectively, the distributions of the numbers n_i and the weights w_i of the different molecular species with respect to their molecular weights. (Cf. Fig. 1.) As is apparent in the above formu-

FIG. 1.

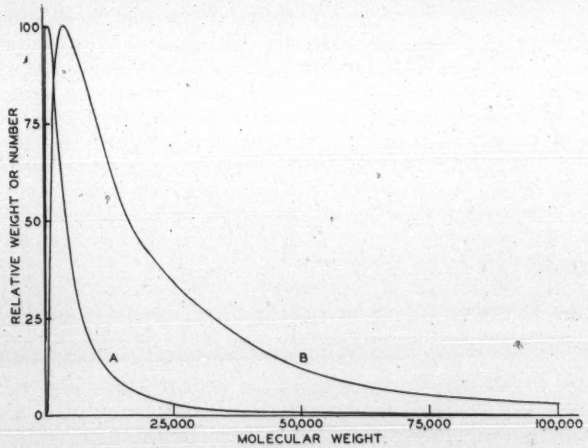

Mutual Relation of Number-Distribution (*A*) and Weight-Distribution (*B*) Curves. These curves represent calculations by Lansing and Kraemer (8) for a gelatin, fitted to the logarithmic probability distribution. β, the non-uniformity coefficient, equals 1.7. The modes of the number and weight curves, respectively, are 1000 and 4200. The number-average, weight-average, and C-average molecular weights are, respectively, 9800, 36000, and 150,000.

lation, the "weight-distribution" of molecular weight is obtained by multiplication of the dependent variable (usually ordinates) of the "number-distribution" (or "molecular

weight-frequency") curve by the corresponding independent variable (or abscissa). Those familiar with statistical analysis will recognize the "number-average" molecular weight as the common, arithmetical mean molecular weight; they will also observe that $\Sigma M_i n_i$ and $\int_0^\infty M \cdot f_n(M) \cdot dM$ in equations (1) and (1*a*) represent the first moment of the number-distribution curve with respect to the ordinate at $M = 0$; $\int_0^\infty f_n(M) \cdot dM$ and $\int_0^\infty f_w(M) \cdot dM$ (or $\int_0^\infty M \cdot f_n(M) \cdot dM$), represent, respectively, the areas of the number-distribution and the weight-distribution curves (i.e., the total number N and the total weight W of material); and M_n, as the arithmetical mean molecular weight, defines the abscissa for the center of gravity of the number-distribution curve.

Since distribution curves are normally expressed on a relative basis with the total area of the curve set equal to 1 or 100, it is evident that the volume- and weight-distribution curves are identical when the specific volume of the particles in the mixture is constant. Only in exceptional cases can one determine molecular or particle weights when this is not so. If the mixture contains a quite limited number of polydispersed components (say 2–4) and the optical properties differ suitably (usually in spectral transmission), it is theoretically possible to distinguish the single components in the ultracentrifuge and thereby to define the individual average molecular weights in spite of differences in specific volumes, provided the latter are known.

Having designated the molecular weight corresponding to the center of gravity of the number-distribution-of-molecular-weight curve as the "number-average molecular weight," we may logically name the corresponding average derivable from the weight-distribution-of-molecular-weight curve as the "weight-average molecular weight." This average is defined by the expression:

$$(2) \qquad M_w = \frac{\Sigma M_i^2 n_i}{\Sigma M_i n_i} = \frac{\Sigma M_i w_i}{\Sigma w_i} = \frac{\Sigma M_i w_i}{W}.$$

The first fraction represents the ratio of the second moment to the first moment (relative to the frequency axis) of the number-distribution-of-molecular-weight curve; the numerator of the second fraction represents the first moment of the

weight-distribution-of-molecular-weight curve, and the first moment of the weight curve equals the second moment of the number curve. In terms of continuous functions:

$$(2a) \qquad M_w = \frac{\int_0^\infty M^2 \cdot f_n(M) \cdot dM}{\int_0^\infty M \cdot f_n(M) \cdot dM} = \frac{\int_0^\infty M \cdot f_w(M) \cdot dM}{\int_0^\infty f_w(M) \cdot dM}.$$

It may be shown (7, 8) that the weight-average molecular weight is obtained by Staudinger's viscosity method, when it is applicable.

Sedimentation equilibrium in the ultracentrifuge yields, under favorable conditions, both number-average and weight-average molecular weights, and, in addition, a "C-average" molecular weight [2] defined by the relations (6, p. 342, 8)

$$(3) \qquad M_C = \frac{\Sigma M_i^3 n_i}{\Sigma M_i^2 n_i} = \frac{\Sigma M_i^2 w_i}{\Sigma M_i w_i}$$

or, for continuous functions:

$$(3a) \qquad M_C = \frac{\int_0^\infty M^3 \cdot f_n(M) \cdot dM}{\int_0^\infty M^2 \cdot f_n(M) \cdot dM} = \frac{\int_0^\infty M^2 \cdot f_w(M) \cdot dM}{\int_0^\infty M \cdot f_w(M) \cdot dM},$$

[2] "C-average" molecular weight is admittedly not a self-explanatory term for what might be called the third-moment molecular weight, meaning thereby the ratio of the third-moment to the second-moment of the number-distribution curve. Since there are so many different types of average values and most of them cannot be identified with any property or experimental technic, it seems best to use as abbreviations simple letters. We originally referred to the "C-average" as the "Z-average," owing to the fact that the "Z-average" was found to result quite directly from the refractive-index records of sedimentation equilibria, in which the scale-displacement values have generally been designated as Z-values. We would suggest, as a convention, that the series of average values corresponding to the first, second, third, etc. moments of a number-distribution curve be designated by the successive letters of the alphabet. Thus the "number-average" could also be designated the "A-average"; the "weight-average" is also the "B-average," etc. As we shall see, some average values involve powers of other average values, e.g., one could refer to Green's D-average diameter (p. 8) as the A1-average-volume. For such complicated quantities, however, it would be preferable to avoid the confusion of involved abbreviations.

where $M_i^3 n_i$ and $M_i^2 w_i$ are, respectively, the third moment of the number-distribution-of-molecular-weight curve, and the second moment of the weight-distribution-of-molecular-weight curve. The C-average molecular weight locates the center of gravity of the curve representing the distribution of $M_i w_i$ (products of molecular weight and weight fraction) with molecular weight. Theoretically, average molecular weights involving higher moments can be calculated from ultracentrifuge data, but, generally, experimental errors accumulate too rapidly to justify the use of moments higher than the third for the weight-distribution curve.

In the above instances, the category or independent variable according to which the classification of the mixture of molecular or particle sizes is considered is M, the molecular or particle weight. Each average value is then, in effect, derived directly from a corresponding distribution curve or statistical table. For the number-average particle weight, the dependent variable for the corresponding distribution curve is the number n_i of particles or molecules in the category or class having a particle weight between M_i and $M_i + dM$. For the weight-average particle weight, the dependent variable of the corresponding distribution is the weight w_i of material in the successive categories; and for the C-average weight, the dependent variable of the corresponding distribution is the quantity $M_i w_i$. In each instance, then, the average molecular or particle weight is the arithmetical mean for the corresponding distribution curve, the "average" weight being the molecular weight locating the ordinate about which the corresponding distribution curve will balance.

These relationships may be generalized by considering that the independent variable for a distribution function or statistical table descriptive of a mixture may be any quality either descriptive of geometrical size or shape, or representing any property which is a function of geometrical size or shape. Thus, the independent variable may be particle radius, diameter or length, surface, weight, volume, axial ratio, etc., or it may be any function of one of these quantities that is descriptive of the magnitude of a physical or chemical property by which the various molecular species or particles in the mixture could be classified, e.g., light absorption coefficient,

viscosity coefficient, diffusion coefficient, sedimentation coefficient, specific reaction constant, etc. In other words, as independent variable, any property may be used which provides a *potentially continuous* basis for classification of the individual particles or molecules in the mixture. The dependent variable, on the other hand, summates the total amount of one of these descriptive qualities associated with one class of molecules or particles which are uniform, within the limits set by the mode of classification, with respect to the quality or property determining the magnitude of the dependent variable per particle or molecule. The dependent variable may be any one of the quantities mentioned above in connection with the independent variable, or any desired function of them, *summated over all the particles or molecules in the given class.* To be of any practical value in the estimation of averages for mixtures, the total effect for any group of molecules or particles must be additive, that is, equal to the sum of the effects for the individual particles. If we then call the independent variable Φ and the dependent variable Ψ, the "average" value or arithmetical mean Φ for the function $\Psi = f(\Phi)$, corresponding to the averages already mentioned, is defined by the expressions:

$$(4) \qquad \Phi_\Psi = \frac{\Sigma \Phi_i \Psi_i}{\Sigma \Psi_i} = \frac{\int_0^\infty \Phi \cdot f(\Phi) \cdot d\Phi}{\int_0^\infty f(\Phi) \cdot d\Phi}$$

and Φ_Ψ may be designated as the "Ψ-average Φ." That is, the arithmetical mean of Φ, with respect to Ψ, is the value Φ_Ψ about which the moment of the distribution curve $\Psi = f(\Phi)$ is zero, or the mean square of the deviations of Φ from Φ_Ψ is a minimum.

This generalization may be clarified by specific applications already in use. In connection with the specification of particle diameters for fine powders, Perrot and Kinney named and defined the following quantities (11):

$$(5a) \qquad \Sigma nd/\Sigma n = \text{number-average diameter},$$

$$(5b) \qquad \Sigma nd^2/\Sigma nd = \text{length-average diameter},$$

$$(5c) \qquad \Sigma nd^3/\Sigma nd^2 = \text{surface-average diameter},$$

$$(5d) \qquad \Sigma nd^4/\Sigma nd^3 = \text{volume-average diameter},$$

$$(5e) \qquad \frac{k}{\Sigma nd^3/\Sigma nd^2} = \text{specific surface}.$$

Our nomenclature is in agreement with this scheme. In accordance with it, the specific surface could also be designated as the reciprocal of the surface-average diameter, or as the volume-average reciprocal-diameter, multiplied by a constant. Similarly, Green's (2) average diameters could be named as follows:

$$(5f) \qquad \Delta = (\Sigma nd^2/\Sigma n)^{\frac{1}{2}}$$
$$= \text{square root of number-average surface.}$$

$$(5g) \qquad D = (\Sigma nd^3/\Sigma n)^{\frac{1}{3}}$$
$$= \text{cube root of number-average volume.}$$

In each instance, the type of average value, which is specified by the compound adjective, is determined by the dependent variable of a distribution curve, and is the denominator in the ratio of two sums, e.g., "number-average," "weight-average," "surface-average," and, as will appear below, "viscosity-average," "light-absorption-average," etc. The quantity averaged is determined by the independent variable of the corresponding distribution curve, and the numerator of the ratio defining the average contains the sum of the products of the dependent and independent variables. If these averages may be considered as basic averages, it may be seen that Green's "average diameters" and the specific surface are not basic averages, but functions of basic averages.

AVERAGE MOLECULAR WEIGHTS BY STAUDINGER'S METHOD.

In determining the type of average value obtained from any given quantity or physical property, one must first calculate the distribution function for the quantity in question, relative to the geometrical characteristic, or a related property, according to which the mixture of molecules or particles can be classified. Thus, in connection with Staudinger's viscosity rule (15), one must first construct a distribution function for viscosity increment versus molecular weight

from the weight-distribution function and the relationship between viscosity and molecular weight, i.e., $(\eta_r - 1)/c = [\eta] = KM$. By multiplying each value of w_i (the fractional weight of material with molecular weight M_i) by the total concentration and the intrinsic viscosity of molecules of weight M_i, we obtain the viscosity increment $(\eta_r - 1)_i$ due to the molecules of weight M_i. That is

$$(\eta_r - 1)_i = c[\eta]_i w_i = cKM_i w_i.$$

These expressions determine the ordinates of the distribution of viscosity increment with molecular weight. The area of the curve, equal to the summation of $(\eta_r - 1)_i$ over all molecular species, gives the total viscosity increment, and dividing by the concentration $c(= c\Sigma w_i)$ and K gives the "average" molecular weight calculated for the mixture, i.e.,

$$(6) \quad \frac{(\eta_r - 1)}{Kc} = \frac{\Sigma(\eta_r - 1)_i}{Kc\Sigma w_i} = \frac{c\Sigma[\eta]_i w_i}{Kc\Sigma w_i} = \frac{Kc\Sigma M_i w_i}{Kc\Sigma w_i} = \frac{\Sigma M_i w_i}{\Sigma w_i}.$$

The third term is evidently proportional to the weight-average value of intrinsic viscosity, $[\eta]_w$, and $[\eta]_w/K$ is equal to the weight-average molecular weight.

It is to be noted that the average molecular weight obtained by application of Staudinger's equation does not bear the same relation to the viscosity-increment distribution curve as exists between, for instance, the number-distribution curve and the number-average molecular weight. The corresponding value, for the viscosity-increment curve, would be designated the viscosity-average molecular weight, and would be defined by the expression

$$(7) \quad M_{\eta s} = \frac{\Sigma M_i(\eta_r - 1)_i}{\Sigma(\eta_r - 1)_i},$$

where $M_{\eta s}$ signifies a viscosity-average value for a material to which Staudinger's viscosity rules apply. Substitution of the values given above for $(\eta_r - 1)_i$ shows that

$$M_{\eta s} = \frac{\Sigma M_i^2 w_i}{\Sigma M_i w_i},$$

which is identical with the C-average molecular weight. This value cannot be calculated from a viscosity determination.

AVERAGE AXIAL RATIO AND PARTICLE SIZE FROM VISCOSITY OF ELLIPSOIDAL PARTICLES.

A somewhat more involved application of the above considerations arises in the interpretation of the viscosity of solutions or suspensions of ellipsoidal particles, which is at present receiving considerable attention from those concerned with the correlation of ultracentrifugal, diffusional and viscosity data for solutions of proteins, polysaccharides and other high polymers. For purposes of illustration, we may utilize the recent calculations of Simha (14) on the viscosity of ellipsoids of various axial ratios. Simha set up the expression $\eta_r - 1 = \nu C_v$, where C_v is the volume-fraction concentration and ν is a coefficient determined by the axial ratio, and has calculated the values of the ν's for axial ratios from 1 to 300. Depending upon whether the ellipsoids are prolate or oblate, ν has different values for given ratios of major to minor axes. Values of ν for oblate or flattened ellipsoids may be designated by ν_f and for prolate or elongated ellipsoids by ν_e. Assuming that all ellipsoidal particles in a given mixture are either oblate or prolate, we may express our basic size-distribution data in the form of volume vs. axial ratio functions

$$v_i = \frac{dv}{d\delta} = f_e(\delta) \qquad \text{and} \qquad v_i = \frac{dv}{d\delta'} = f_f(\delta'),$$

where $\delta = L/d > 1$, $\delta' = d/L > 1$, L is the axis of revolution, d is the equatorial diameter, and subscripts e and f distinguish the two kinds of ellipsoids.

The viscosity increment $(\eta_r - 1)_i$ due to molecules with axial ratio δ_i is equal to $C_v v_i(\nu_e)_i$ and the total viscosity increment for the mixture is therefore given for prolate ellipsoids by

$$\Sigma(\eta_r - 1)_i = C_v \Sigma v_i(\nu_e)_i \tag{8}$$

where v_i is the volume-fraction of all particles or molecular species that possess an axial ratio of δ_i, and $(\nu_e)_i$ is the corresponding viscosity coefficient. (There is a similar equation for ν_f.) The experimental "average" value of ν_e is given

by the expression

$$\text{(9)} \qquad \text{Average } \nu_e = \frac{\Sigma(\eta_r - 1)_i}{C_v \Sigma v_i} = \frac{\Sigma(\nu_e)_i v_i}{\Sigma v_i}.$$

Thus, experimental determinations of ν_e or ν_f lead to volume-average values, which may be represented by the symbols $(\nu_e)_v$ and $(\nu_f)_v$.

In terms of continuous functions, the basic distribution curve for prolate ellipsoids is $dv/d\delta = f_e(\delta)$ and the ordinates of the viscosity-increment distribution curve for a concentration C_v are

$$\frac{d(\eta_r - 1)}{d\delta} = C_v \cdot \nu_e \cdot \frac{dv}{d\delta} = C_v \cdot \nu_e \cdot f_e(\delta),$$

where ν_e is a function $F_r(\delta)$. The total viscosity-increment is therefore

$$\int_0^\infty \frac{d(\eta_r - 1)}{d\delta} \cdot d\delta = C_v \int_0^\infty F_r(\delta) \cdot f_e(\delta) \cdot d\delta.$$

The total volume concentration equals

$$C_v \int_0^\infty \frac{dv}{d\delta} \cdot d\delta = C_v \int_0^\infty f_e(\delta) \cdot d\delta.$$

And the experimental "average" value of ν_e is found to be

$$\text{(10)} \qquad \text{Average } \nu_e = \frac{\eta_r - 1}{C_v} = \frac{\int_0^\infty F_r(\delta) \cdot f_e(\delta) \cdot d\delta}{\int_0^\infty f_e(\delta) \cdot d\delta}.$$

We see therefore that the experimental "average" value of ν_e is really the volume-average value of the function $F_r(\delta)$ relating viscosity coefficient and axial ratio. The final result could have been set down immediately because of the complete parallelism between ν and $[\eta]$, which was discussed above. For a constant specific volume, the volume-average is, as already mentioned, equal to the weight-average value.

The question still remains as to the conclusions that may be drawn concerning definable average values of δ. To find the relationship between volume-average values of ν and δ, consider Simha's tables for ν and δ for prolate and oblate ellipsoids.

Oblate ellipsoids.—With reasonable accuracy (sufficient for illustrative purposes) Simha's ν-values for oblate ellipsoids may be expressed by the equation:

$$\nu_f = 1.40 + 0.675\delta' \tag{11}$$

for values of δ' between 2 and 300 (the maximum value included in Simha's tables). For large values of δ', the constant 1.40 may be ignored and

$$\nu_f \backsimeq 0.675\delta'.$$

Now the volume-average

$$(\nu_f)_v = \frac{\Sigma(\nu_f)_i v_i}{\Sigma v_i},$$

which, in terms of δ', equals

$$\frac{\Sigma 0.675\delta_i' v_i}{\Sigma v_i} = 0.675\delta_v', \tag{12}$$

where δ_v' is the volume-average value of δ' (when $\delta' \gg 1$).

If the various molecular or particle species in the mixture represent a polymer-homologous series differing only with respect to one axis, it is possible to calculate a definite average molecular weight, as well as the volume-average axial ratio. The molecular weight, specific volume and axial ratio are related by the expression $MV/N = \pi Ld^2/6$. If the equatorial diameter is constant, $L = (6V/N\pi d^2)M = k_d M$. Therefore, for oblate ellipsoids with large values of d/L

$$(\nu_f)_v \backsimeq 0.675(d/L)_v = 0.675\left(\frac{d}{k_d M}\right)_v = \frac{0.675d}{k_d}\left(\frac{1}{M}\right)_v \tag{13}$$

and the volume-average value $(\nu_f)_v$ thus permits the calculation of the volume-average value of $(1/M)$ provided d is known. But, as seen above, the volume- or weight-average of $(1/M)$ is given by the expression $\frac{\Sigma w_i \cdot 1/M_i}{\Sigma w_i}$, which is the reciprocal of

$$\frac{\Sigma M_i n_i}{\Sigma M_i n_i \cdot \frac{1}{M_i}} = \frac{\Sigma M_i n_i}{\Sigma n_i}.$$

In other words, for this particular case, the reciprocal of the number-average molecular weight may be calculated from viscosity data.

For a similar system of much flattened ellipsoids, for which L is constant and d varies, $d = k_L(M)^{\frac{1}{2}}$, where $k_L = (6V/N\pi L)^{\frac{1}{2}}$ and the volume-average

$$(14) \qquad (\nu_f)_v \backsimeq 0.675 \left(\frac{k_L M^{\frac{1}{2}}}{L} \right)_v = \frac{0.675 k_L}{L} (M^{\frac{1}{2}})_v.$$

The viscosity measurements in this case, therefore, yield the weight-average square root of molecular weight $(M^{\frac{1}{2}})_v$, provided L is known. In none of these cases is it possible to calculate other types of average values, either of ν, δ' or M, from a single average value of any sort without information regarding the exact distribution function for the sample in question.

When δ' is not very large (say, $\delta' < 150$), then one must take account of the correction constant 1.40. That is, the volume-average value of ν_f is equal to the volume-average value of the quantity $(1.40 + 0.675\delta')$ and the volume-average value of δ' cannot be calculated without knowledge or assumptions concerning the distribution function for the sample. Furthermore, without additional information, no type of average molecular or particle weight is calculable.

Prolate ellipsoids.—For elongated ellipsoids, Simha's values of ν_e can be approximately expressed by the empirical power series:

$$(15) \qquad \nu_e = -2.24 + 1.082\delta + 0.0508\delta^2 - 21.5 \times 10^{-6}\delta^3 \quad (\text{for } \delta > 10)$$

and the volume-average value of ν_e is equal to the volume-average value of the entire series expression. Again, without information regarding the distribution function for the sample, the calculations cannot be carried further.

In an earlier publication (8), we showed the usefulness of a two-parameter logarithmic-probability distribution function for interpreting ultracentrifuge data on size-distribution characteristics of macromolecular mixtures. The same equation had previously been used by Hatch and Choate (4) and

others (1, 9) to express the size-distribution of particulate materials. The function may be written

$$\frac{dw}{dM} = \frac{e^{-0.25\beta^2}e^{-y^2}}{M_0\beta\sqrt{\pi}},$$

where $y = \dfrac{\ln M/M_0}{\beta}$ and $\beta \geq 0$, M_0 is the mode, and β measures the width of the distribution curve. dw is the relative weight of material having molecular weights between M and $M + dM$ and is expressed as a fractional value, i.e., $\int dw = 1$. Applying this equation to the present case we may state the distribution of axial ratios on a volume-fraction basis as follows:

$$v_i = \frac{dv}{d\delta} = \frac{e^{-0.25\beta^2}e^{-y^2}}{\delta_0\beta\sqrt{\pi}} \tag{16}$$

where $y = \dfrac{\ln \delta/\delta_0}{\beta}$, $\delta = \delta_0 e^{\beta y}$, $d\delta = \delta_0\beta \cdot e^{\beta y} \cdot dy$ and δ_0 is the mode of the $dv/d\delta$ vs. δ curve. The viscosity increment for a mixture of concentration C_v with this distribution of δ is

$$\frac{d(\eta_r - 1)}{d\delta} = C_v \cdot \nu_e \cdot \frac{dv}{d\delta}.$$

Substituting values of ν_e and $dv/d\delta$ from equations (15) and (16) and integrating to give the total viscosity increment gives:

$$\int_0^\infty \frac{d(\eta_r - 1)}{d\delta} \cdot d\delta = \frac{C_v}{\delta_0\beta\sqrt{\pi}} \int_{-\infty}^{\infty} [-2.24 + 1.082\delta_0 e^{\beta y} + 0.0508\delta_0^2 e^{2\beta y} - 21.5 \times 10^{-6}\delta_0^3 \cdot e^{3\beta y}] \cdot e^{-0.25\beta^2} \cdot e^{-y^2} \cdot \delta_0 \cdot \beta \cdot e^{\beta y} \cdot dy. \tag{17}$$

Division of eq. (17) by C_v then gives $(\eta_r - 1)/C_v$, or the volume-average value $(\nu_e)_v$. Upon cancelling $\delta_0\beta$ and integrating term by term, the first term becomes

$$-2.24 \int_{-\infty}^{\infty} e^{-(y^2 - \beta y + 0.25\beta^2)} dy$$

$$= -2.24 \int_{-\infty}^{\infty} e^{-x^2} \cdot dx \quad (\text{where } x = y - 0.5\beta;\ dx = dy)$$

$$= -2.24\sqrt{\pi}.$$

The second term becomes

$$1.082\delta_0 \int_{-\infty}^{\infty} e^{-(y^2-2\beta y+0.25\beta^2)}dy$$
$$= 1.082\delta_0 \int_{-\infty}^{\infty} e^{-x^2}\cdot e^{0.75\beta^2}\cdot dx \quad (\text{where } x = y - \beta;\ dx = dy)$$
$$= 1.082\delta_0\sqrt{\pi}e^{0.75\beta^2}.$$

The remaining terms are integrated similarly and

$$(18)\quad (\nu_e)_v = -2.24 + 1.082\delta_0 e^{0.75\beta^2} + 0.0508\delta_0^2 e^{2\beta^2} - 21.5 \times 10^{-6}\delta_0^3 e^{3.75\beta^2}.$$

When the material is homogeneous, $\beta = 0$ and $(\nu_e)_v$ reduces to the value of ν_e given by equation (15). The greater the heterogeneity, the larger is the discrepancy between $(\nu_e)_v$ and the value of ν_e corresponding to the value of δ_0, the mode of the volume-distribution curve.

It may be shown (8) that $M_w = M_0 e^{0.75\beta^2}$ if the weight-distribution of molecular weight is given by the logarithmic probability distribution function. Similarly, for constant specific volume, $\delta_v = \delta_0 e^{0.75\beta^2}$ and $(\nu_e)_v$ may be expressed in terms of the volume-average axial ratio. That is:

$$(19)\quad (\nu_e)_v = -2.24 + 1.082\delta_v + 0.0508\delta_v^2 e^{0.5\beta^2} - 21.5 \times 10^{-6}\delta_v^3 e^{1.5\beta^2}.$$

Accordingly, the volume-average axial ratio can be calculated from viscosity data and the volume-average value of ν_e provided the distribution function (or β) is known.

When the distribution is the logarithmic probability one, the effect of heterogeneity may be shown by taking the difference of equations (15) and (18) or (15) and (19), comparing $(\nu_e)_v$ for a mixture and ν_e for homogeneous ellipsoids having an axial ratio equal to either the modal or the volume-average axial ratio of the mixture. Since the exponents of equation (18) are so large, we shall consider only the difference between equations (15) and (19), which is:

$$(20)\quad (\nu_e)_v - \nu_e = 0.0508\delta^2(e^{0.5\beta^2} - 1) - 21.5 \times 10^{-6}\delta^3(e^{1.5\beta^2} + 1).$$

Equation (20) indicates that for certain values of δ and β, the value of $(\nu_e)_v - \nu_e$ is zero; for a given β, the value of $(\nu_e)_v - \nu_e$

is positive for sufficiently small values of δ and negative for relatively large values of δ. The following table illustrates the implications of equation (20) for various conditions:

TABLE I.

β	δ for $(\nu_e)_v - \nu_e = 0$	Fractional Difference $[(\nu_e)_v - \nu_e]/\nu_e$			
		$\delta = 10$	$\delta = 50$	$\delta = 100$	$\delta = 300$
0.5	128	0.046	0.059	0.025	−0.19
1.0	279	0.24	0.38	0.36	−0.17
1.5	162	0.73	1.04	0.69	−1.88
2.0	37	1.75	40	−9.1	−48

Column 2 gives the values of δ at which the sign of $(\nu_e)_v - \nu_e$ changes from positive to negative, and columns 3, 4, 5, and 6 show the relative difference between the volume-average $(\nu_e)_v$ for a mixture and ν_e for a homogeneous system when the axial ratio of the latter is equal to the volume-average axial ratio of the former. It is apparent that the difference between $(\nu_e)_v$ and ν_e is relatively small (e.g., < 10 per cent.) for values of β not exceeding 0.5 and for axial ratios not exceeding 100. Otherwise, the discrepancy is considerable, increasing with both β and δ. The values shown in the table for the largest values of β and all of the values for $\delta = 300$ are strictly speaking only illustrative, and may be seriously in error since they depend upon the rather unlikely assumption that the power series expressed by equation (15) can be extrapolated for appreciable distances beyond $\delta = 300$, at which point Simha's table of values ceases. Similarly the values for $\delta = 10$ are somewhat erroneous because the above power series was not adjusted to fit Simha's values for axial ratios below 10. In general, therefore, one must be rather cautious in drawing inferences concerning definable average axial ratios based on viscosity determinations unless the volume distribution of δ is known.

For polymer-homologous series involving stiff, rod-like molecules (crudely represented by cellulose (6, p. 430, 8)), the value of the thickness may be considered constant, and, as shown above, $L = k_d M$. The relationship between $(\nu_e)_v$ and M_v, the weight- (or volume) average molecular or particle

weight is then given by the following expression, assuming validity of the logarithmic-probability distribution:

$$(21)\quad (\nu_e)_v = -2.24 + \frac{1.082k_d}{d}\cdot M_v + \frac{0.0508k_d^2}{d^2}\cdot M_v^2 e^{0.5\beta^2} - \frac{21.5\times 10^{-6}k_d^3}{d^3}\cdot M_v^3\cdot e^{1.5\beta^2}.$$

For this particular case, β is the non-uniformity coefficient for both the volume distribution of molecular weight, as well as for the axial ratio.

AVERAGE PARTICLE SIZES FROM LIGHT ABSORPTION.

Another application of these considerations deserving attention is that involving turbidity, light scattering and resulting light absorption, since these properties are often used to estimate particle size. In addition, these properties are concerned in the ultracentrifugal analysis of suspensions by the light absorption method.

For very small transparent particles, within the range of Rayleigh's law, the specific absorption coefficient κ (per unit volume concentration) due to light-scattering is given, for a single wave length, by the expression.

$$(22)\quad \kappa = kv = k^1 d^3,$$

where v is the volume and d is the diameter of the individual particles, and k and k^1 are constants of proportionality depending upon the wave length, refractive indices, and the factor converting d^3 to volume. For a dilute mixture of particles of different sizes, the total absorption coefficient of the suspension is $\Sigma\kappa_i c_i$ where c_i is the ordinate of the volume distribution of diameter curve for the mixture. The "average" specific absorption coefficient is the volume- (or weight) average absorption coefficient or $\frac{\Sigma\kappa_i c_i}{\Sigma c_i}$, and the "average" volume of the particle is given by

$$(23)\quad \text{Ave. volume} = \frac{\Sigma\kappa_i c_i}{k\Sigma c_i} = \frac{k\Sigma v_i c_i}{k\Sigma c_i} = \frac{\Sigma v_i c_i}{\Sigma c_i}.$$

This is the volume- (or weight) average particle volume,

corresponding to weight-average molecular weights discussed above. The corresponding "average" diameter is

$$\text{Ave. diameter} = \sqrt[3]{\frac{\Sigma \kappa_i c_i}{k^{\mathrm{I}} \Sigma c_i}} = \sqrt[3]{\frac{\Sigma c_i d_i^3}{\Sigma c_i}}; \tag{24}$$

i.e., the cube-root of the volume-average cubed diameter, or simply, the cube-root of the volume-average particle volume.

When the particles are appreciably larger than the wave length λ employed (e.g., $d > 2\lambda$), the light absorption k_p for n particles is proportional to their projected area (16, 17):

$$k_p = k^{\mathrm{II}} n d^2 = \frac{k^{\mathrm{III}} v}{d},$$

where v is the volume of the particle. The specific absorption coefficient (per unit volume concentration) is therefore

$$\kappa = k_p/c = k^{\mathrm{IV}}/d. \tag{25}$$

For a mixture of sizes, the total absorption coefficient of the suspension is, as above, equal to $\Sigma \kappa_i c_i$, and the "average" specific absorption coefficient is $\frac{\Sigma \kappa_i c_i}{\Sigma c_i}$. The corresponding "average" diameter is given by $\frac{k^{\mathrm{IV}}}{\kappa} = \frac{k^{\mathrm{IV}}}{\Sigma \kappa_i c_i / \Sigma c_i}$, which is equal to $\frac{\Sigma c_i}{\Sigma c_i / d_i}$ and might logically be designated the reciprocal of the weight-average reciprocal-diameter. By replacing c_i by $n_i d_i^3$, a more informative designation is obtained, namely, $\frac{\Sigma n_i d_i^3}{\Sigma n_i d_i^2}$, or the surface-average diameter (or C-average diameter).

For general purposes of particle-size specification, the weight (or volume) average diameter is probably the most useful, although the most appropriate for a particular application of the powder in question depends upon the relation between particle size and the effect the powder is desired to confer in its application. Since the weight-average diameter is $d_w = \frac{\Sigma n_i d_i^4}{\Sigma n_i d_i^3}$, the surface-average diameter, given by the light absorption method with relatively coarse particles, is

smaller than the desired value. On the other hand, the average diameter by the light absorption method with very small particles may be expressed as

$$\sqrt[3]{\frac{\Sigma n_i d_i^6}{\Sigma n_i d_i^3}}.$$

It may be shown that this average diameter is equal to the cube root of the product of the three average diameters d_B, d_C, d_D where

$$d_B = \frac{\Sigma c_i d_i}{\Sigma c_i} = \text{the weight-average diameter,}$$

$$d_C = \frac{\Sigma c_i d_i^2}{\Sigma c_i d_i} = \text{C-average diameter,}$$

$$d_D = \frac{\Sigma c_i d_i^3}{\Sigma c_i d_i^2}.$$

Since each of these averages is equal to or greater than the weight-average diameter, the average diameter obtained from light absorption measurements, with very small particles, is therefore larger than the desired weight-average diameter, the difference depending upon the size-distribution function.

It is well known that the light absorption per unit projected area for transparent particles increases rapidly with decreasing particle size as the diameter approaches the wave length of the light used (12) and must pass through a maximum before joining the curve representing very small particles. The projected area light absorption **K** is

$$\mathbf{K} = \frac{k^{\mathrm{V}} \kappa c}{n d^2}, \tag{26}$$

which, for large particles, is a constant, and for very small particles equals $k^{\mathrm{VI}} d^4$. At the maximum of the curve, the slope is again zero, so that just at the maximum, as at large particle sizes, an average particle size by light absorption measurements would correspond to a surface-average diameter. In the region between the maximum of the curve and the horizontal section referring to particles much larger than the wave length, the projected area adsorption varies

proportionally with a negative power of the diameter, and an average particle size here would be smaller than the surface-average diameter. On the small particle size of the maximum, before the curve reaches the Rayleigh region, the projected area absorption varies with an increasing power of diameter, the exponent being 0 at the maximum and gradually increasing to 4 in the Rayleigh region. In this region, therefore, the average particle diameter increases from a surface-average diameter through the volume-average diameter to the cube root of the volume-average volume. In the whole region between the Rayleigh region and large particles, one can specify the meaning of a light absorption measurement of average particle size only if the function relating specific absorption coefficient and particle size is known.

When an ultracentrifuge analysis is made in the conventional way, by the light absorption method, one obtains directly the distribution curve for the product $\kappa_i c_i$ versus particle diameter, or, if desired, versus particle volume. In earlier papers (10) we have called such curves weight-optical distribution curves, although to be consistent with the more explicit nomenclature of this paper, they should be designated as light-absorption vs. particle diameter (or volume) distribution curves. The mean particle diameter derived directly from an ultracentrifuge distribution curve is given by $\frac{\Sigma \kappa_i c_i d_i}{\Sigma \kappa_i c_i}$ and should be called the light-absorption average diameter; other average diameters, e.g., the volume-average diameter, cannot be calculated without knowing the function relating light absorption and particle diameter.

These examples illustrate the general methods to be employed in interpreting measurements for physical or physico-chemical properties of mixtures of molecular species or of particles differing in size or other properties. The primary requirement for the validity of these methods is additivity of the effects of the individual molecules or particles for any property under consideration. It is evident that average values of any quality may be quite misleading, depending upon the degree of heterogeneity occurring in the mixture, and, in general, caution must be exercised in making use of average values for some property of a mixture, which

are calculated without explicit information concerning the distribution of the property among the components of the mixture.

BIBLIOGRAPHY.

1. DRINKER, *J. Ind. Hyg.*, **7**, 305 (1925).
2. GREEN, J. FRANK. INST., **204**, 712 (1927).
3. FORDYCE, LOVELL AND HIBBERT, *J. Am. Chem. Soc.*, **61**, 1905, 1910 (1939).
4. HATCH AND CHOATE, J. FRANK. INST., **207**, 369 (1929); **215**, 27 (1933).
5. HATCH AND CHOATE, J. FRANK. INST., **210**, 793 (1930).
6. KRAEMER, in "The Ultracentrifuge" by Svedberg and Pedersen, Oxford Press, 1940.
7. KRAEMER AND LANSING, *J. Phys. Chem.*, **39**, 153 (1935).
8. LANSING AND KRAEMER, *J. Am. Chem. Soc.*, **57**, 1369 (1935).
9. LOVELAND AND TRIVELLI, J. FRANK. INST., **204**, 193, 377 (1927).
10. NICHOLS, KRAEMER AND BAILEY, *J. Phys. Chem.*, **36**, 326 (1932).
11. PERROT AND KINNEY, *J. Am. Ceram. Soc.*, **6**, 417 (1923).
12. RICHARDSON, *J. Appl. Phys.*, **11**, 653 (1940).
13. SIGNER, in "The Ultracentrifuge" by Svedberg and Pedersen, Oxford Press, 1940.
14. SIMHA, *J. Phys. Chem.*, **44**, 25 (1940); *Science*, **92**, 132 (1940).
15. STAUDINGER, "Die hochmolekularen organischen Verbindungen," Springer, Berlin, 1932.
16. TOLMAN *et al.*, *J. Am. Chem. Soc.*, **41**, 575 (1919).
17. WALTON, *J. Ind. Hyg.*, **18**, 689 (1936).

Get Altitude Conditions in "Strato-Chamber."—(*Refrigerating Engineering*, Vol. 40, No. 3.) Research engineers at the Boeing Aircraft Company, where the first fleet of "altitude-conditioned" substratosphere transport planes has recently been completed, have equipped themselves with a laboratory which permits airplane development work to reach not only the substratosphere but the stratosphere itself. A steel "strato-chamber" complete with air locks, superchargers, vacuum pumps, control valves and even refrigeration, re-creates on the ground the conditions of supercharged flight up to altitudes of 40,000 ft. and higher. The stratosphere begins at approximately 36,000 ft. where the atmospheric pressure is less than $\frac{1}{4}$ the pressure at sea level. In the test chamber, engineers can "fly" in a few minutes time to any desired altitude, either with comfortable supercharged air conditions or with oxygen masks and no supercharging. Within the sealed walls of this chamber, bedecked with instruments and test devices, are contained both the rarefied, frigid outside air of the stratosphere and in another compartment the warmed, normal air of a modern supercharged airplane cabin. The experimental and development work made possible by this chamber can be made of far-reaching importance to both commercial and military aviation. In the commercial field, practical supercharged operations at moderately high altitudes, up to 20,000 ft. have already been demonstrated by the Boeing Stratoliners of TWA and Pan American Airways. By means of automatic supercharging apparatus which increases the density of the air circulating in the cabin, the Stratoliner maintains air conditions in the cabin equivalent to 8,000 ft altitude when the plane is flying as high as 15,000 ft., and maintains approximately 12,000 ft. altitude conditions when the plane is actually 20,000 ft. above sea level. In the military field, high altitude operation has already been pushed above these heights through the use of oxygen equipment instead of supercharged cabins, and research work that is being carried on in the interests of crew comfort and efficiency at extremely high altitudes is of major importance.

R. H. O.

THEORY OF THE HALFTONE PROCESS.

I. THE PENUMBRA THEORY.*

BY

J. A. C. YULE.

This is the first of a series of papers on the theory of the halftone process. Subsequent papers will deal with the diffraction theory, tone reproduction, combined exposures with different apertures, flash exposures, resolving power, and the relationship of dot sharpness to emulsion characteristics.

For many years, there has been much confusion and controversy concerning the optics of halftone dot formation. The correct solution of the problem was stated qualitatively by Ives [1] in 1898 when he said:

"There has been some dispute as to whether we should speak of the dots as pinhole images or as geometric shadows. The fact is that they are both; it is perfectly obvious that we are dealing with geometric shadows, but it is equally true that any pinhole image is made up of geometric shadows—so we have here a distinction without a difference—except, perhaps, in degree, as the relative size of the aperture to the image distance varies, and as the disturbing effects of diffraction are made more or less manifest."

Since that time many false statements have been made, and few appear to have understood the subject as well as Ives. Little attempt seems to have been made to check the various theories experimentally. In the present paper, an attempt will be made to clarify the problem and to present evidence in support of the solution. The question to be answered is as follows:

Under given conditions of camera aperture, screen distance, etc., what will be the distribution within a halftone dot of the light reaching the sensitive emulsion; or in other

* Communication No. 786 from the Kodak Research Laboratories.

[1] F. E. Ives, *London Technical Education Gazette*, 5, 2–17, No. 51 (January, 1899).

words, what will be the light intensity at any given point on the emulsion, and how will this be related to dot formation and tone reproduction?

Two theories have been proposed to account for the light distribution—the penumbra and diffraction theories. The advocates of the penumbra theory usually claim [2] that diffraction plays a negligible part in dot formation, while the supporters of the diffraction theory often regard the penumbra theory as totally incorrect.[3,4] It will be shown in the present paper that the penumbra theory only explains the observed results for coarse screens and abnormally short screen distances and is inadequate to account for the results obtained under the conditions used in practice. It is hoped that this discrepancy can be accounted for by diffraction. The two theories do not actually conflict with each other; one is merely a more accurate statement of the other.

The penumbra theory is based on the approximately true assumption that light travels in straight lines, and may be worked out quantitatively by means of a simple geometrical construction. Although the method has been described in detail by Calmels and Clerc [2,5] and by Fruwirth,[4] it will be briefly reviewed here:

When a halftone screen is set up in the usual way at a certain distance in front of the plate in a camera, the intensity at any point P (Fig. 1) in the plane of the emulsion depends upon the area of the camera aperture which is visible from that point. A microscopic observer at the point P would see a partial eclipse of the aperture, as shown in Fig. 1*B*. In this particular case, 75 per cent. of the camera aperture would be visible, so the intensity at P is 75 per cent. of what it would be with the screen removed. Similar calculations may be made for all points in the plane of the emulsion.

After these intensities have been calculated, points of equal intensity may be joined to form contours, "isophotes," or "isolux lines," as in Figs. 2 to 6. In these figures, the size

[2] L. P. Clerc, "Ilford Manual of Process Work," London, p. 102 (1926).

[3] M. Levy, *Process Photogram*, 3, 20–22 (1896).

[4] A. Fruwirth, *American Photo-Engraver*, 27, 369–377, No. 5 (May, 1935).

[5] H. Calmels and L. P. Clerc, *Process Engraver's Monthly*, 15, 217–219, 249–252, 267–270 (1908).

and shape of the projection, onto the plane of the emulsion, of the lens aperture through the center of the screen opening and of the screen opening through the center of the lens aperture, are shown by dotted lines.

FIG. 1.

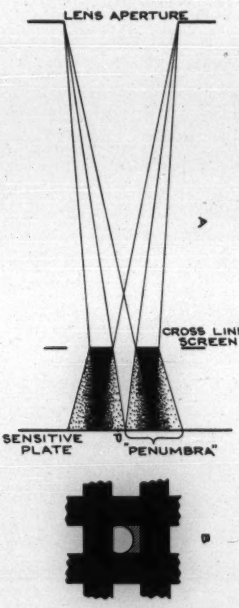

Optics of halftone screen according to penumbra theory.

According to the penumbra theory, it follows from simple geometry that if

$$\frac{\text{lens aperture}}{\text{camera extension}} \times \frac{\text{screen distance}}{\text{screen opening}}$$

remains constant, exactly the same light distribution in the halftone dots will be obtained on a larger or smaller scale,

FIG. 2.

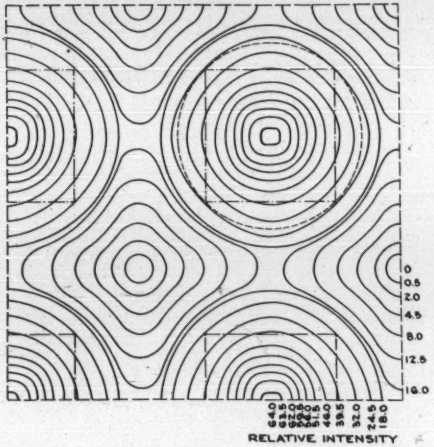

Dot formation according to penumbra theory. Calculated for round aperture with diameter equivalent to diagonal of screen opening. (Courtesy of A. Fruwirth.)

FIG. 3.

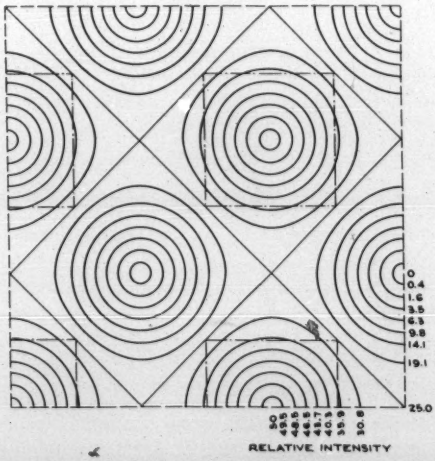

Dot formation according to penumbra theory. Calculated for square aperture with side equivalent to diagonal of screen opening. (Courtesy of A. Fruwirth.)

FIG. 4.

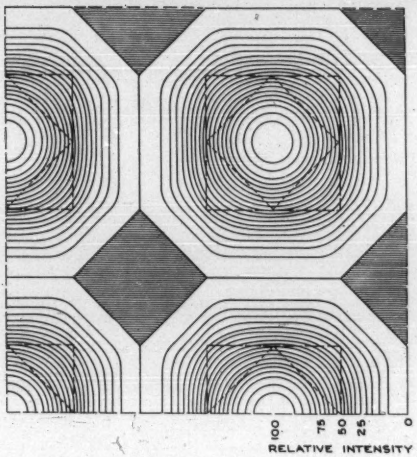

Dot formation according to penumbra theory. Calculated for square aperture with diagonal equivalent to side of screen opening. (Courtesy of H. Calmels and L. P. Clerc.)

FIG. 5.

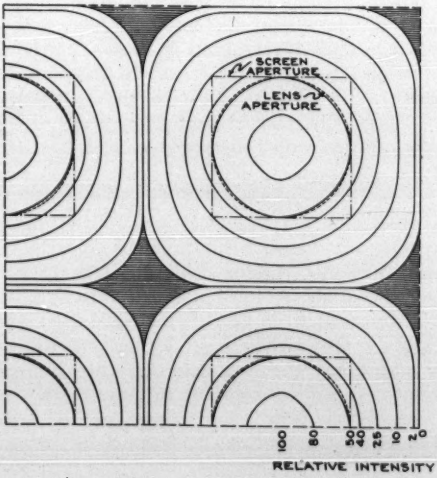

Dot formation according to penumbra theory. Calculated for round aperture with diameter equivalent to side of screen opening.

FIG. 6.

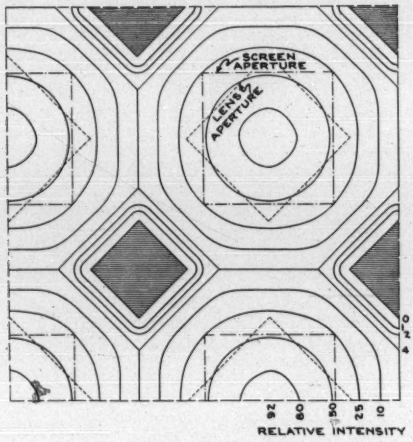

Dot formation according to penumbra theory. Calculated for square aperture of same area as aperture for Fig. 5.

according to the fineness of the screen. Any screen distance may be chosen, and the required light distribution obtained by using the appropriate lens aperture for this screen distance. The penumbra theory gives rise to the following "screen equation" as a guide for choosing the most suitable lens aperture for a given screen distance:

$$\frac{\text{lens aperture}}{\text{camera extension}} = \frac{\text{screen opening}}{\text{screen distance}}.$$

The screen opening refers to the length of the side (or according to some workers, the length of the diagonal) of a single square aperture of the screen. The theoretical basis for this equation is supposed to be that it will give the smallest and sharpest shadow dot, although, in actual fact, this argument is strictly valid only if a diamond aperture is used, i.e., a square orientated the same way as the screen opening.

According to the diffraction theory, on the other hand, each screen is shown to have a definite focus and should

always be used at this distance, although the diffraction theory says nothing about the size of aperture which should be used.

Clerc and Fruwirth have calculated the light distribution with round and square apertures of such size that the light intensity just reaches zero at the darkest point in each dot (Figs. 2 and 3). This is given by the screen equation when the diagonal, instead of the side of the screen opening, is used in the equation. Calmels and Clerc have also given a diagram for a square aperture of one-quarter of this area (Fig. 4). Calculations have now been made for the round aperture given by the screen equation, using the *side* of the screen opening (Fig. 5), and also for a square aperture (Fig. 6) of the same area as the round one used in Fig. 5. In these figures, the sizes of the lens apertures and screen openings are represented by dotted lines.

The obvious method of checking the light distribution experimentally would be to set up a microphotometer behind the screen and to measure the brightness at various points in the dot. Since no suitable instrument for this purpose was available, an indirect method was used:

If a photographic material of infinitely high contrast and resolving power were available, it would remain clear for all exposures up to a certain critical value, and all exposures above this would blacken it. If such a material were placed behind the halftone screen, an exposure could be chosen which would just give minute black dots at the points of maximum illumination. Doubling the exposure would, of course, give larger dots, and the boundaries of these dots would coincide with the lines of half the maximum illumination. As the exposure is increased further, the dots would increase in size, always having boundaries coinciding with lines of equal illumination, until a point was reached where the dots closed up completely. This would correspond to the point of minimum illumination of the dot. Photomicrographs could then be made of the dots in this screen negative, and, by tracing the outlines of the dots obtained with different exposures, a contour map of the light distribution might be constructed (Figs. 6 to 8). Alternatively, a microscope might be used to project the images of the dots in the screen negative

directly onto a sheet of ground glass, on which the dot outlines could be traced with a pencil.

Experimentally, the exposures can all be made simultaneously through a step-tablet, on a material with the highest available contrast; if this is not high enough, a contact print on a high contrast material can be made from the screen negative. For the tests plotted in Figs. 7 to 9, the following conditions were used:

TABLE I.

Fig.	Screen Ruling.	Screen Distance (Optical).	Camera Extension.	Aperture.	Corresponding Penumbra Calculation.
		inches	inches	inches	
7	60	0.265	35	1.1 round	Fig. 5
8	60	0.265	35	0.95 square	Fig. 6
9	120	0.29	35	0.5 round	Fig. 5

FIG. 7.

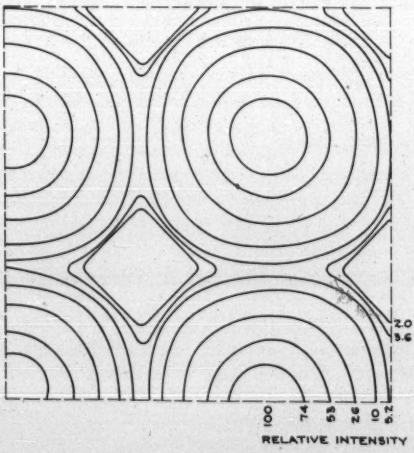

Dot formation, observed with 60-line-per-inch screen and round lens aperture,

$$\frac{\text{screen distance}}{\text{screen opening}} = \frac{\text{camera extension}}{\text{aperture diameter}} = 32.$$

The same geometrical conditions as Fig. 5.

FIG. 8.

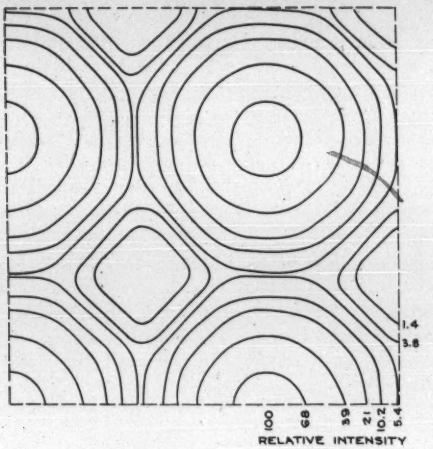

Dot formation, observed with 60-line-per-inch screen and a square aperture of the same area as for Fig. 7. The same geometrical conditions as Fig. 6.

FIG. 9.

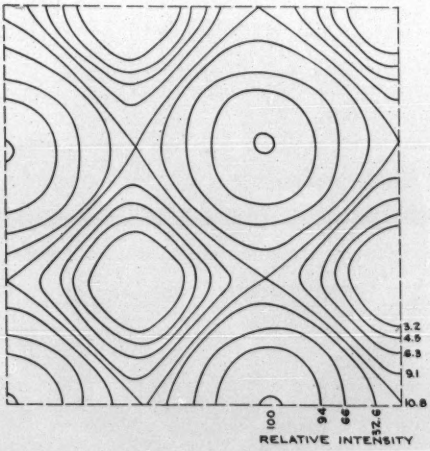

Dot formation, observed with 120-line-per-inch screen,

$$\frac{\text{screen distance}}{\text{screen opening}} = \frac{\text{camera extension}}{\text{aperture diameter}} = 70.$$

The same geometrical conditions as Fig. 5.

The step-tablet is placed in the object plane of the camera, since its diffusing properties would affect the light distribution in the dot, if placed between the lens and the plate.

Eastman Contrast Process plates, developed in D-8 for 2 minutes, were used for the negatives. Tests were also made with plates dyed with tartrazine to reduce spreading of light in the emulsion. To obtain sharp dots, a contact print was made from the negative on Ortho Kodalith film, and developed to a gamma of about 7.0. Unfortunately, no comparison exposure was made with the screen removed, so that the intensity values are only relative. An arbitrary value of 100 units was assigned to the center of the dot, in Figs. 7 to 9.

A comparison of Figs. 7 and 10 with Fig. 5, and of Figs. 8 and 11 with Fig. 6 shows that the dot shape corresponds excellently with the calculated patterns, when extremely short screen distances, large apertures, and coarse screens are used.

While this type of chart is very useful for showing the shapes of the dots, the relative sizes of the dots, which are

FIG. 10.

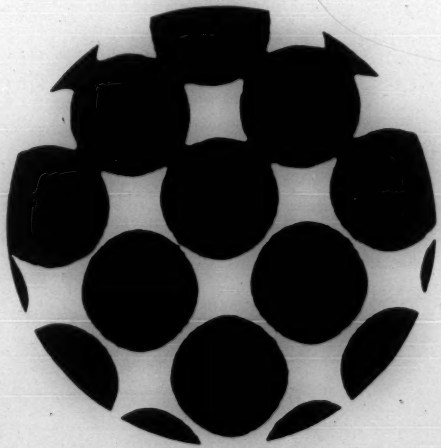

Photomicrograph of dots obtained as in Fig. 7.

FIG. 11.

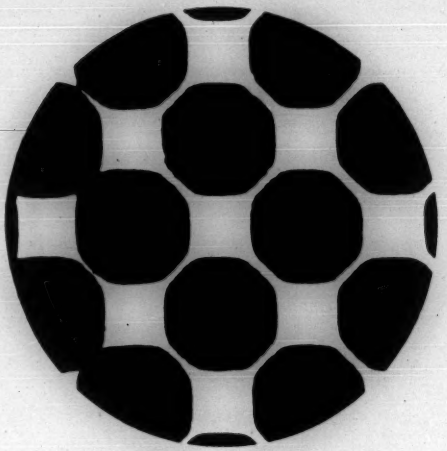

Photomicrograph of dots obtained as in Fig. 8.

FIG. 12.

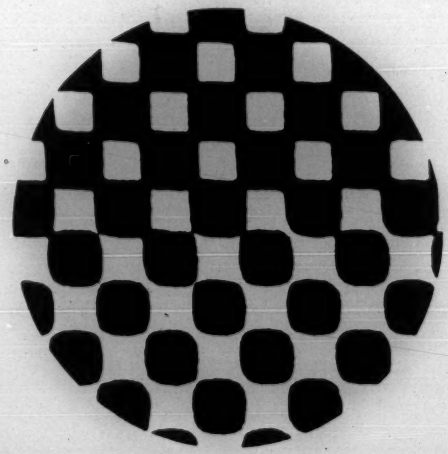

Photomicrograph of dots obtained as in Fig. 9.

even more important, are more clearly shown by plotting in a different way. The areas enclosed within the isolux lines can be measured and plotted against the intensity at the corresponding line. The areas are expressed as a fraction of the total area per screen element. From Figs. 2 to 6, the curves of Fig. 13 are thus obtained. The areas for the experi-

FIG. 13.

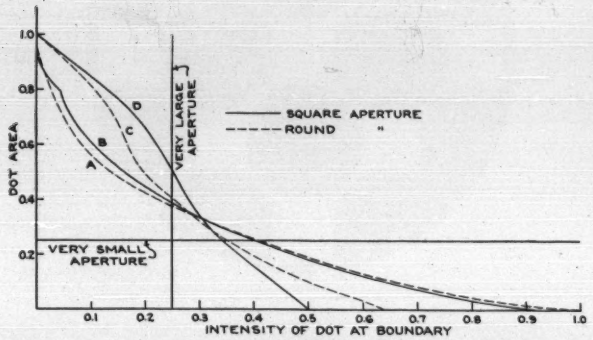

Relationship of dot area to intensity at edge of dot, calculated from penumbra theory. Intensities are calculated as fractions of the intensity with no screen. Dot areas represent the areas enclosed by lines of equal intensity, calculated as fractions of the total area per screen element. Calculated from (*a*) Fig. 5, (*b*) Fig. 6, (*c*) Fig. 2, (*d*) Fig. 3.

mental curves were determined by measuring the density of the screen negative or positive, subtracting 0.02 (the fog density), and converting to per cent. transmission. In addition, curves have been added for very small and very large lens apertures. In the former case, the intensity drops from one to zero at the boundary of a square of area 0.25, corresponding to the screen opening, while with a very large aperture, the screen pattern is completely lost, and there is a uniform intensity of 0.25 over the whole plate. Other apertures, of course, give curves intermediate between these extreme cases.

In Fig. 14, the curve corresponding to the screen equation (Fig. 4) with a round aperture is compared with the experimentally determined curves for these conditions. It will be seen that, with short screen distances and large apertures,

the experimental and calculated curves check within the limits of experimental error, except in the regions of very low intensity. Too much light has penetrated into these regions. It was thought at first that this might be due to light scattered in the emulsion. The tests were, therefore, repeated with plates dyed with tartrazine, to eliminate light scattering. However, the curves for both dyed and undyed plates correspond closely, so that the discrepancy must be due to light scattered in some other way—from the inside of the camera, by the screen, or by a slight diffraction effect.

FIG. 14.

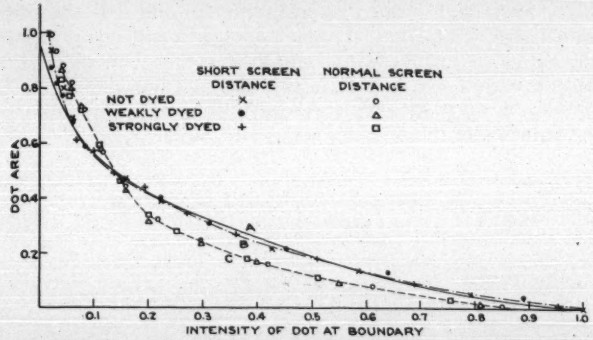

Relationship of dot area to intensity at edge of dot, determined by experiment, geometrical conditions as in Figs. 5, 7, and 9. Curve *A* calculated from penumbra theory, as in Fig. 5. Curve *B* experimental, with short screen distance and coarse screen, as in Fig. 7. Curve *C* experimental, with normal screen distance and fine screen as in Fig. 9.

On the other hand, when a fine screen and a normal screen distance are used, the discrepancy between the penumbra calculation and the observed results is large, both as regards dot shape (compare Figs. 5, 9, and 12) and dot area (Fig. 14).

Photomicrographs of some of the actual dots from which Figs. 7, 8, and 9 were traced are shown in Figs. 10, 11, and 12, respectively.

According to the penumbra calculations, Figs. 5, 7, and 9 should all be identical, and the curves of Fig. 14 should all coincide, since all conform to the screen equation. The marked discrepancy when using a fine screen (Fig. 9 and

Curve *C*, Fig. 14) cannot be explained without taking diffraction into account.

TONE REPRODUCTION.

The most important function of the light distribution in the dot is to control the tone reproduction curve of the halftone print. The density of a region in a halftone depends on the density and area of the individual dots,[6] according to the equation:

$$D = -\log [aR_b + (1 - a)R_w],$$

where R_b and R_w are the reflectances or transmissions of the black areas and clear areas, respectively, and a is the fractional area occupied by the black dots. In halftone printing, typical values are $R_w = 1.00$ and $R_b = 0.04$. This represents an ink with a density of 1.4 printed on white paper whose density is taken as zero. A conversion table obtained by substitution of these values is given in Table II.

TABLE II.

Conversion of Area to Integrated Density of Halftone when Maximum Density = 1.4.

$D = -\log (1 - 0.96a)$.

% Black Area.	0.	1.	2.	3.	4.	5.	6.	7.	8.	9.
0	0	0	0.01	0.01	0.02	0.02	0.03	0.03	0.04	0.04
10	0.05	.05	.06	.06	.06	.07	.07	.08	.08	.09
20	.09	.10	.10	.11	.12	.12	.13	.13	.14	.14
30	.15	.16	.16	.17	.17	.18	.19	.19	.20	.21
40	.21	.22	.23	.23	.24	.25	.26	.26	.27	.28
50	.29	.29	.30	.31	.32	.33	.34	.35	.35	.36
60	.37	.38	.40	.41	.42	.43	.44	.45	.46	.47
70	.49	.50	.51	.53	.54	.55	.57	.59	.60	.62
80	.64	.65	.67	.69	.71	.74	.76	.78	.81	.84
90	.87	.90	.93	.97	1.01	1.06	1.11	1.16	1.23	1.30
100	1.40									

By measuring the areas enclosed within lines of equal illumination in Figs. 2 to 6 and converting these to density by means of this equation or by the conversion table, the density obtained with varying exposures can be determined and, hence, the tone reproduction curve. For instance,

[6] A. Murray, J. FRANK. INST., 221, 721–744 (1936).

suppose we have a light distribution corresponding to Fig. 3, and the sensitivity of the emulsion is such that a pinpoint dot is just obtained with unit exposure. From the chart, it is seen that the relative intensity at the center of the dot is 50. Now, suppose the exposure is doubled. The dot boundaries will then coincide with the isolux line of half the intensity, i.e., 25. This line encloses an area equal to half the total

FIG. 15.

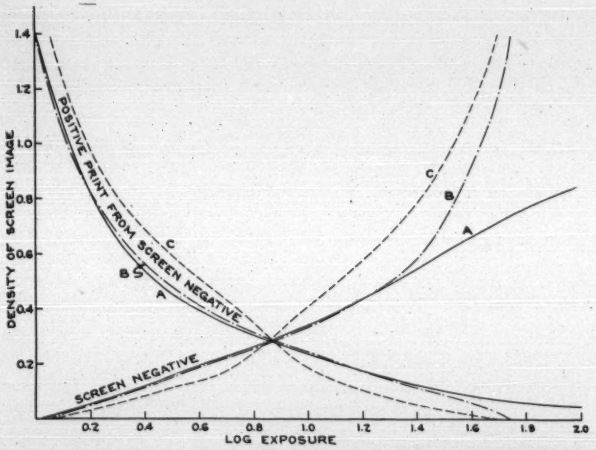

Tone reproduction curve, calculated and observed, geometrical conditions as in Figs. 5, 7, and 9. Curve *A* calculated from penumbra theory as in Fig. 5. Curve *B*, experimental, with short screen distance and coarse screen as in Fig. 7. Curve *C*, experimental, with normal screen distance and fine screen as in Fig. 9.

area. From the table we see that this gives a density of 0.29. Redoubling the exposure gives an area (enclosed by the isolux line 12.5) of 0.808. This corresponds to a density of 0.81. The complete tone reproduction curve (i.e., density vs. log exposure) can be plotted from these values, or conversely, if a tone reproduction curve is given, the area enclosed by the isolux lines can be plotted.

In Fig. 15, the results shown in Fig. 14 have been converted to tone reproduction curves as just described.

As Tritton and Wilson have pointed out,[7] when density instead of dot area is plotted, the shape of the curve depends upon whether a screen negative or a screen positive is used, since the relationship between the densities of screen negatives and screen positives is not linear. When using dot area, the only difference between negative and positive is that the curve is turned upside down, i.e., all areas in the negative are subtracted from 1.00 to give the dot area in the positive. The curves of Fig. 15 have, therefore, been plotted for both negatives and positives. It has been assumed throughout that the solid black of the halftone has a density of 1.4, and actual densities of screen negatives and positives were converted to this scale by adding 4.2 to their per cent. transmission, reconverting to density, and adding 0.02 to the density. The results obtained in this way have a much closer relationship to actual halftone prints than the true densities as measured in a densitometer.

All these results point to the fact that diffraction must be taken into account in order to explain the phenomena. The quantitative treatment of the diffraction theory is considerably more complicated and will be left to a later paper.

SUMMARY.

A method of calculating the tone reproduction curve of a halftone from the light distribution behind the halftone screen, or vice versa, is described. The actual light distribution is found to check satisfactorily with the distribution calculated from geometrical optics, i.e., penumbra theory, when coarse screens and abnormally short screen distances are used, except in the regions of very low light intensity. With fine screens and normal screen distances, both dot shape and tone reproduction differ markedly from the calculated results and can only be explained by the effects of diffraction.

[7] F. J. Tritton and E. T. Wilson, *Phot. J.*, 79, 396–407 (1939).

ANTICIPATORY TRIGGERING DEVICES FOR LIGHTNING AND STATIC INVESTIGATIONS.

BY

B. F. J. SCHONLAND, F.R.S., AND J. S. ELDER,

The Bernard Price Institute of Geophysical Research, Johannesburg.

1. It is now well known that a lightning discharge to ground begins, if the ground is not provided with an exceptionally tall conductor, with a stepped leader streamer travelling from cloud to earth.[1] This leader process consists of intermittent and rapid extensions of the streamer over distances ranging from 50 to 100 meters. The steps occur at intervals of 30 to 100 μ-secs. and take place over a pre-ionised trail provided by a slow pilot streamer moving ahead of the step streamer and periodically caught up by it. Light, electromagnetic waves and sound, are radiated during this process as a series of intermittent pulses of very short duration, for a time which ranges from .001 to .07 second, and is most frequently close to .01 sec. Since these pulses precede the main return portion of the first stroke, they may be utilised to trigger recording devices of various kinds in anticipation of the rest of the discharge. Such anticipatory triggering devices are of obvious value in the study of various aspects of the lightning discharge, which must otherwise be investigated as transient phenomena whose time of occurrence cannot be predicted. Two successful applications of these triggers are described below in the hope that they may be of use to others working in this field.

2. *Application to Photographic Studies of Lightning in Daylight.*—Studies of lightning with cameras provided with fast moving lenses or films have previously been restricted to the night hours, since the lenses must be left open and the film continuously exposed until such time as a suitable discharge occurs. As the majority of thunderstorms take

[1] Schonland, B. F. J., Malan, D. J., and Collens, H., *Proc. Roy. Soc. A.*, **152**, 1935, 595; McEachron, K. B., JOURN. FRANKLIN INST., **227**, 1939, 149.

place in the day time, the yield from such studies is not large. There is, moreover, no certainty that the mechanism of the discharge by day is identical in all respects with that observed at night.

In the application of anticipatory triggering to this problem, the camera shutter is automatically opened by the

FIG. 1.

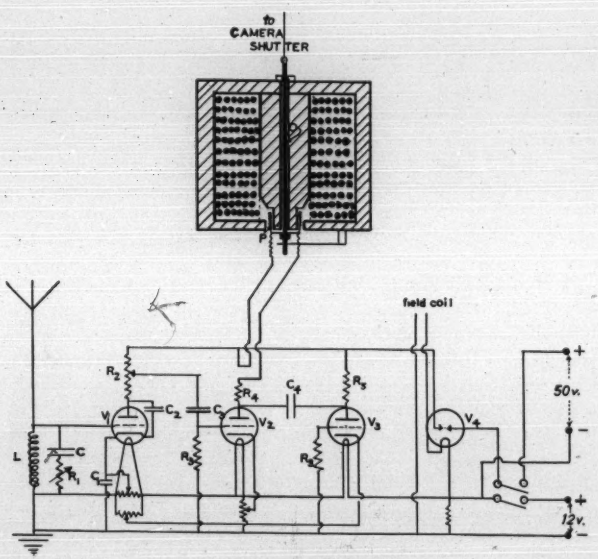

Daylight lightning trigger.
R_1, R_2, R_3, R_4, R_5; 250, 5 × 10^4, 2 × 10^5, 100, 4000, ohms.
C_1, C_2, C_3, C_4; 1, 0.1, .01, 16, mfds.
V_1, V_2, V_3; *AC/2HL, GT1A, GT1A.*

stepped leader process to the first stroke of the discharge and closed by the usual spring timing device half a second later. This time is sufficient to include all the strokes or partial discharges of most lightning flashes. If the camera is provided with a continuously rotating drum carrying a recording film of length 2 meters and the lens aperture covers a portion

of the film 2 cms. square, the actual exposure to daylight of each part of the film is .005 seconds. Since the daylight intensity is low during most thunderstorms the amount of fogging is not serious and the details of the luminous development of the discharge can often be recorded as well by day as by night.

The arrangement developed for this purpose is shown in Fig. 1. The series of radio wave pulses described in §1 is received on an aerial system, tuned by the circuit *LCR* to respond fairly evenly to frequencies from 30 to 100 K.C./sec.

V_1 produces a rectified signal which causes the gas-filled tube V_2 to strike and pass a current through the coil *P*. The second gas-filled tube V_3, which normally carries current is extinguished by the striking of V_2 for a time set by C_4 and R_5, about half a second. When V_3 recovers its plate potential and strikes again it extinguishes V_2 and resets the trigger.

The coil *P* is mounted at the end of a light aluminium rod *O* and can move downwards into the air gap of a powerful electromagnet. Current from V_2 reaches it through flexible leads. The rod *O* is attached by a short piece of fishing-line to the trigger of the fast Compur shutter of the camera. The striking of V_2 causes a strong downward acceleration of *P* and the shutter opens about .002 seconds later. Controls are provided, as shown in Fig. 1, for altering the sensitivity of the device by changing either the biases on V_1 and V_2 or the output from V_1. These are useful for preventing more distant storms from actuating the trigger. Some degree of directivity for the same purpose can be obtained by making *L* a large frame aerial.

Experience with this device shows that it always opens the camera shutter before the first leader process is over. Some examples of daylight records obtained with it are shown in Fig. 2. The film speed employed was 2 meters per second, and time is measured horizontally from left to right.

Flash 1 of this figure consists of two strokes, *a* and *b*, which though mounted together occurred at an interval of .015 secs., 3 cms. apart on the moving film. Stroke *a* is complex, having five components. Stroke *b* has a clearly marked dart leader, visible to the left of the main return portion. Flashes 2 and 3 consisted of single strokes only

and both show faint subsequent components to the right of the main return portion.

Most thunderstorms give rise to more discharges within the cloud than to ground. Since the former usually consist of stepped leader streamers, they also open the camera

FIG. 2.

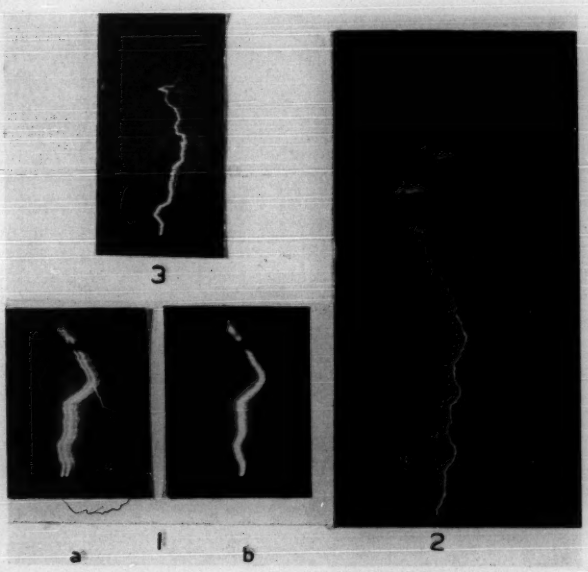

Photographs of lightning taken on moving film in daylight.

shutter and produce daylight fogging which may be troublesome if no ground flash occurs for some time. In practice fair pictures—sometimes reversed—can be obtained after eight such exposures. An improvement would be to operate the trigger from a photoelectric cell. This would have the additional advantage that it would only respond to discharges which are in the field of view of the camera.

The maximum working range of the device is from 10 to 20 kms. depending upon the intensity of the daylight prevailing at the time. The first successful model was operated in December, 1936. That described here was designed by British Electricon Ltd. on lines suggested by one of us.

3. *Application to Studies of the Wave-form of Static Disturbances Produced by Distant Lightning.*—Anticipatory triggering can be used to advantage in the study of an important class of natural static, that produced by a lightning flash to ground. Such disturbances are found to begin, as is the case with near lightning, with a lengthy train of pulses from the first stepped leader process,[2] even though the source is as much as 4500 kms. away. By using the leader train the beam of the cathode-ray oscillograph employed to record such transient wave-forms can be switched on at very high intensity just before the arrival of the main disturbance and be switched off automatically .04 second later when it has passed by. The beam intensity used can therefore be very much higher and the writing-speed faster than is possible in continuous recording. The method also involves great saving in photographic film material.

Since neither man-made static nor all forms of lightning origin have such stepped leader processes preceding them, it is desirable to prevent such forms, which would trigger the equipment late, from operating the device. Use was therefore made of the differences between the leader and the subsequent main disturbances to eliminate triggering from the latter alone. The intervals between successive pulses in the leader wave-form in static range from 20 to 50 μ-secs. (ionospheric reflection plays a part in such distant propagation) and their period does not exceed 20 μ-secs. The main disturbance which follows carries pulses or "waves" of much longer period, increasing from 60 μ-secs. at the start to 600 μ-secs. at the end. It seldom has superimposed transients of periods as short as are common on the leader; if these occur they are confined to the first 100 μ-secs. of the main portion and do not form trains. On the other hand, the leader pulses form trains lasting as long as .01 seconds. The

[2] Watson-Watt, R. A., Herd, J. F., and Lutkin, F., *Proc. Roy. Soc. A*, 162, 1937, 267; Lutkin, F., *Proc. Roy. Soc. A*, 171, 1939, 285.

trigger was therefore designed to respond to such short period trains and to be insensitive to the longer period main disturbances even if these were of much larger amplitude.

Fig. 3 shows the main trigger circuit. The aerial circuit was in this case aperiodic, producing potential differences across R_1 proportional to the rate of change of the electric field in the disturbance. These were amplified by three

FIG. 3.

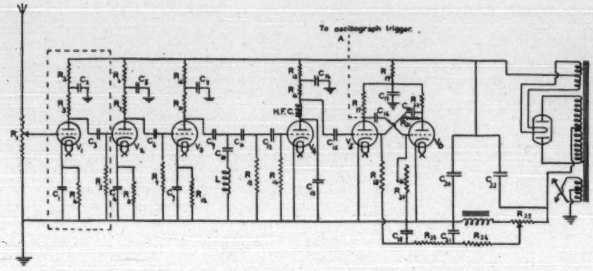

Static wave-form trigger (pt. 1).

$R_{1,2,3,6,7,19,11,14,15}$	25,000 ω	$R_{17,22}$	250,000 ω
$R_{4,8,13}$	750 ω	R_{18}	100,000 ω
$R_{5,9,21}$	500,000 ω	R_{20} variable from 0.1–10 MΩ	
R_{12}	10,000 ω	$R_{23,24}$	50,000 ω
$R_{15,16}$	5,000 ω	R_{25}	1,000 ω

$C_{1,4,7}$	.25 μF	C_{13}	.5 μF
$C_{2,5,8,14,17}$	1.0 μF	C_{15}	.02 μF
$C_{3,6}$	.001 μF	$C_{16,19}$	.01 μF
$C_{9,11,12}$	.0002 μF	$C_{18,21}$	2.0 μF
C_{10}	.0005 μF	$C_{20,22}$	3.0 μF

L is a pair of Varley "Nicore" H.F. chokes connected in parallel.

R–C coupled stages, one of which could be cut out if desired. The output from V_3 was fed into a high-pass filter cutting off at 50 kc./sec., suitably matched to V_3 and terminated by R_{12}. The voltages across R_{12} were rectified by the grid of V_4. The time constant of the grid circuit was made short (40 μ-secs.) so that a succession of pulses was necessary for the grid to be held negative for any appreciable time. The time constant of the plate of V_4 on the other hand was made long, about a millisecond. The combined action of the filter

and the grid and plate circuits of V_4 was therefore to make this tube respond most effectively to the prolonged trains of high-frequency waves or pulses constituting the stepped leader portion of the static disturbances.

The output from V_4 was fed to V_5, which with V_6 forms an asymmetrical modification of the well-known multivibrator circuit. V_5 was normally biassed back to cut-off while V_6 carried current. Positive output from V_4 passed to the grid of V_5 causes this tube to carry current, a process quickly built up by the cross-connections to and from V_6 until in a short time V_5 carries a large current and V_6 is cut off. The

FIG. 4.

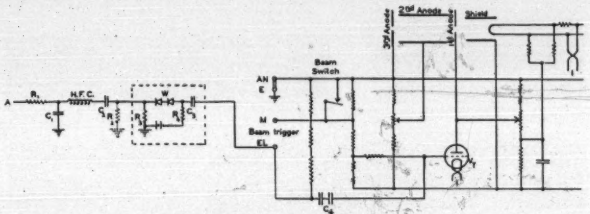

Static wave-form trigger (pt. 2).

R_1 = 2,000 ω	C_1 = .005 μF.
R_2 = 1.0 Megohm	C_2 = 2.0 μF.
$R_{3,4}$ = 0.1 Megohm	C_3 = .05 μF.

resulting drop in the plate potential of V_5 was used to operate an oscillograph beam-trigger *via* the lead A, as shown in Fig. 4.

Figure 4 shows how the negative triggering impulse was applied to the beam control of an oscillograph. From A it passed first through a radio-frequency by-pass circuit to prevent the radiation of r.-f. transients by the line as a result of the sudden action of the trigger. Next it passed through an arrangement designed to keep any A.C. mains-frequency ripple from the oscillograph away from the trigger circuit of V_5 and V_6. This consisted of two metal rectifiers, W, normally kept non-conducting by a bias of a few volts which could be overcome by the triggering impulse. After passing through this the negative impulse operated the beam control of a Cossor oscillograph, passing through C_4 to the

grid of V_7 and raising automatically the potential of the first anode of the oscillograph tube.

The sensitivity of the device could be controlled by the input potentiometer R_1 and the variable bias R_{25} (Fig. 3).

FIG. 5.

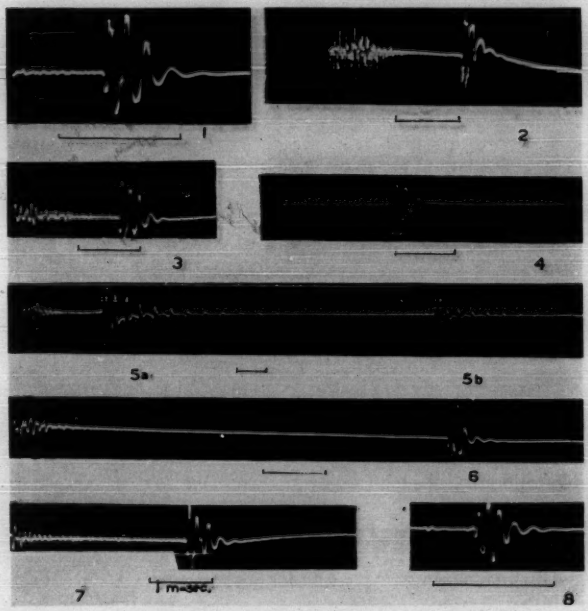

Static wave-forms recorded with anticipatory trigger.

The duration of the "on" period of the oscillograph beam was controlled by varying the time constant of the grid circuit of V_6 by means of R_{20}.

This device was found satisfactory in recording static from flashes more than 2000 kms away. Some records obtained with it are shown in Fig. 5.

The length of the line below each record in Fig. 5 represents 1 millisecond. Faster recording speeds could have been employed but were not wanted in the investigation for which these records were made. The records show that the trigger operated the recording beam in each case well in advance of the main disturbance, some of the leader train being caught by the recorder as well. 2 and 6 are good examples of type β leaders, whose amplitude is large at the start of the process and falls off later. 5*a* and 5*b* are a pair of night static forms from the same flash, the beam being "on" long enough to catch the second stroke of the flash. 8 is a static form from a flash at a distance of 1700 kms. In such more distant forms the main disturbance begins with small (ground) waves which would be lost if the trigger did not anticipate them.

Take It Easy.—(Stone and Webster Bulletin Vol. 8, No. 3.) To measure the hazard involved in driving at various speeds the Travelers Insurance Company has developed the "danger unit" which is defined in stopping distance, roll over, vertical fall and turning radius. Under average conditions the distance an automobile moves after its driver has decided to make an immediate stop varies as the square of its speed. A "danger unit" equals 35 to 40 feet of stopping distance. A car traveling at 25 miles per hour can be stopped in this distance, while in stopping from 50 miles per hour it will travel between 140 and 160 feet, the equivalent of four "danger units." Nearly one full danger unit is added when the speed of a car is increased from 45 to 50 miles per hour. In case of too sharp a turn a car will sometimes roll over once for each "danger unit" it carries. Thus it may roll over once at 25 miles per hour, twice at 35, and perhaps nine times at 75. It is well to remember that only in the luckiest accident can the driver cling to the inside of the rolling car as it does its 3 turns at 45. Striking a solid object at 25 will do a car about the same damage as if it had been driven off a two story building. Encountering a stone wall at 50 will be just as serious as if it dropped from 4 × 2 stories, or 8 stories. When Captain George Eyston was doing 300 miles per hour and more on the dry salt beds of Utah, his engine was packing energy into his car with such industry that it was adding one "danger unit" for each mile of increased speed. Had he hit a solid stone wall he and his machine would have been smashed as irreparably as if he had driven off a 3000 foot ledge into Grand Canyon. Each added "danger unit" caused the car to require a longer turning radius. Thus a car can make only $\frac{1}{4}$ as sharp a turn at 50 as at 25; 1/9 as sharp a turn at 75 as at 25. It is because a car can be turned very little at high speed that many serious accidents occur on curves and when passing.

R. H. O.

THE FLUX EXPANSION FROM THE LUMINOUS DISC.

BY

ALFRED A. WOHLAUER.

Every engineer desires to simplify his mathematical auxiliaries, in order to arrive at his figures in the most practical manner and with the least effort. The illuminating engineer who is employing extended light sources at an increasing rate today, faces a rather disconcerting situation as the formulæ for exact calculation are complicated and unwieldy.

It therefore occurred to the writer that it might be helpful to study the expansion of the flux by charting it in accordance with the available material.[1] This may then perhaps result in a comprehensive picture of the flux action and produce suitable relations for engineering use. Incidentally it may lead to a more profound conception of the time-honored term, the candle power. The latter is fundamentally correct, as formulated, only in connection with the luminous point or with the sphere, while for other luminous surfaces it can be applied but in approximation.

The following is the result of this study and tends to depict the flux expansion from a luminous disc and to compare the procedure with the one customary and correct for spherical expansion.

As an introduction it seems to be well to retrace the action of the luminous sphere as a basis for comparison. Such a sphere, illustrated by the circle S of Fig. 1, emits its flux uniformly in a spherical expansion as if it originated from an imaginary luminous particle located in the center O. This performance is in reality quite a composite affair as it is the result of smaller spherical impulses sent out by the innumerable particles forming the sphere. How they combine and

[1] When this article was prepared the work of E. P. Hyde, *Bulletin of National Bureau of Standards*, Vol. 3, and also Ziro Yamauti's, *Researches of Electrotechnical Laboratory*, Vols. 148 and 339, were known to the writer, but not Gershun's Book, the "Light Field," which appeared in English Translation by Parry Moon, *Journal of Math. & Phys.*, Vol. XVIII, May 1939.

FIG. 1.

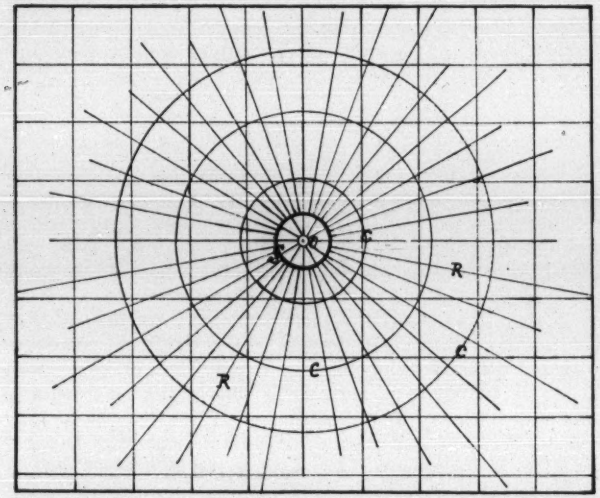

Flux expansion from Luminous Sphere.

what individual intensity they possess is immaterial here. In any event the concentric circles *C* in Fig. 1 represent spheres of constant illumination; they are "Equilux or Isolux-spheres." These spheres are partitioned by radial lines *R*, also called "rays" which of course are not endowed with a physical existence. They encompass solid angles having their apex in the center *O*. Within these solid angles the expanding flux retains a constant value; so does its spherical density, called luminous intensity and expressed in candle power. The latter is measured however as an illumination at unity distance from the center without reference to its physical characteristic as an intensity, except that it is normal to the expanding equilux spheres. In the plane of the paper these relations can only be pictured by a cross section through the sphere, as shown in Fig. 1. Thus the angles formed by the rays represent conical zones usually of equal plane angle, as in the regular polar coordinate papers.

These observations are not new and are indicated here principally for a comparison with the relations and similarities applying to luminous sources of different shape, such as the luminous disc, illustrated by *AB* of Fig. 2. Here the condi-

FIG. 2.

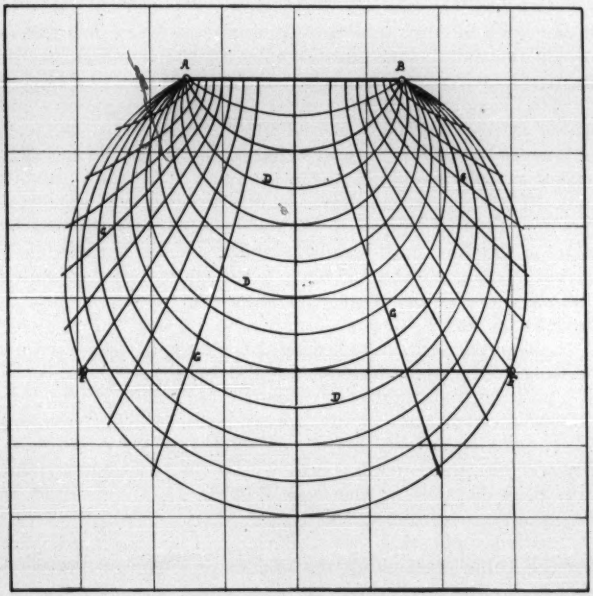

Flux expansion from Luminous disc.

tions are as follows: It has been shown [2] that the flux from a circular disc expands in such a manner that it distributes uniformly upon any sphere on which the disc forms a small circle. These spheres are "Equilux-spheres," but they are not concentric, as in the case of the luminous sphere, but while the flux is expanding, the center of the spheres moves along the vertical axis forward from the disc.

[2] A. S. McAllister, *Electrical World*, Vol. 56, Page 1356.

Now if the area of the disc is divided into a number of equal circular areas and likewise the surface of each equilux sphere into the same number of equal circular zones, the surfaces connecting the dividing lines enclose solids of equal and constant flux just as the conical zones of the sphere. This is illustrated in Fig. 2 in which AB is the common chord of all circles which represent the equilux spheres. In order to divide each equilux sphere into equal zones, one has but to divide the axis below the disc into equal parts so that the segments of the sphere (circles in Fig. 2) have equal height.

The lines which then connect the various segments and which represent surfaces of revolution, indicated by the lines G, correspond to the "rays" of the luminous sphere and thus describe a picture of the flux expanding from the luminous disc. They of course have again no physical existence, but they may be likened to lines of force, marking the direction of the flux and possibly its intensity. In fact their curvature is such that at each point thereof the so called illumination vector (vector of maximum flux density) is tangent thereto.

As the space encompassed by these lines encloses constant portions of the expanding flux to all intersecting areas, one is in a position to evaluate the average flux density or illumination produced on such an area. For instance the flux covering the circular space indicated by EF of Fig. 2 comprises three zones of the total of nine into which the disc and spheres have been divided and therefore will amount to one third of the total flux emitted by the disc.

Further application for calculation will be gone into below, but the value of charting the flux in the manner described may be well demonstrated here by a comprehensive representation afforded thereby of the law of reciprocity.

This law which has long been established[3] states that the flux delivered by one surface upon another is equal to the flux delivered by the second upon the first, if the second were luminous instead of the first, but with the same brightness as the first. Figure 3 explains this and its significance rather forcibly: The construction of the lines G of the expanding

[3] Lambert, "Photometria." German Translation by Anding, 1892, Pages 73 and 82.

flux in either case is only indicated, but sufficient to show that the part of the flux indicated by *ab* and coming from *AB* for illumination of *CD* is exactly equal to the part *cd* that would reach *AB* from *CD*. If the brightness would have the same value in both cases, then the fluxes would be alike, but of course not the illumination.

FIG. 3.

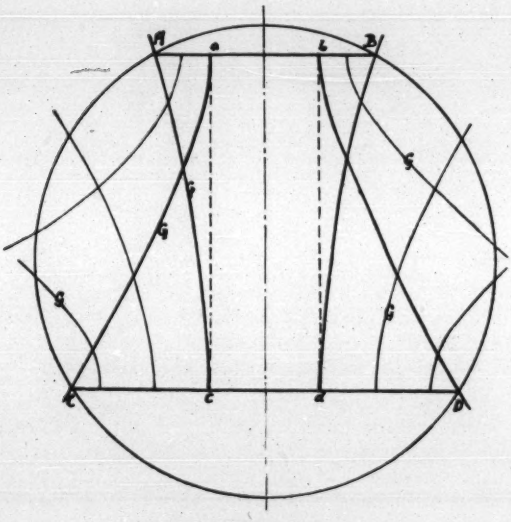

Pictorial explanation of reciprocity law.

Before going into the matter further it seems to be incumbent to establish the character of these curves *G* or of the solids of revolution represented by them. They are apparently hyperbolas, and one of the important characteristics of a hyperbola is the property that the difference of the distances of any point of the curve from two fixed points (Foci) be constant.

FIG. 4.

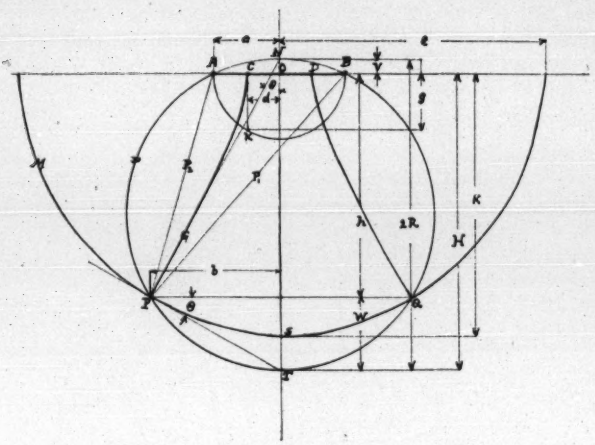

Geometrical relations of equilux sphere, hyperbola and ellipse.

In Fig. 4 which is a cross section through the center of the disc AB, showing one Equilux Sphere $APQB$ and one solid $CPQD$ formed by rotation of curve G and indicated by CP:

a = radius of the disc,
b = horizontal distance of a point P from the vertical axis,
h = vertical distance of P from plane of disc,
p_1 = long distance of P from the edge of the disc; $p_1 = PB$,
p_2 = short distance of P from edge of disc; $p_2 = PA$,
R = radius of Equilux Sphere through P,
H = vertical distance of south pole of equilux sphere from plane of disc,
w = vertical distance of south pole from horizontal plane through P,
v = vertical distance of north pole of sphere from plane of disc,
d = distance of origin of hyperbola from center axis; $d = OC$,
g = vertical distance of C from sphere having radius equal a; $g = CK$.

Now it has been shown,[4] that the flux delivered from the disc upon another circular area parallel thereto, such as for instance upon a horizontal plane through P, thus having a radius equal b, is

$$F_P = \tfrac{1}{4} \cdot B' \pi (p_1 - p_2)^2, \tag{1}$$

wherein B' is the flux density of the flux emitted by the disc; and in as much as this flux has been made a constant part of the total and equal to

$$F_d = B' \cdot \pi d^2$$

by making

$$\frac{H}{w} = \frac{h + w}{w} = \frac{a^2}{d^2}, \tag{2}$$

there is

$$\tfrac{1}{2}(p_1 - p_2) = d = \text{constant} \tag{3}$$

and the curve CP and thus also DQ are hyperbolæ and A and B their foci. The equation of the hyperbola is

$$\frac{b^2}{d^2} - \frac{h^2}{g^2} = 1. \tag{4}$$

If it comes to determine the value of the horizontal illumination at P just described by the ordinates b and h, one has to start from the well known formula

$$E_H = \frac{a^2}{a^2 + H^2} \cdot B' \tag{5}$$

in which H is not known, unless the corresponding equilux sphere is available. From simple geometrical relations, there is

$$a^2 = v(h + w) = v \cdot H. \tag{6}$$

There is further according to (2)

$$d^2 = \frac{a^2 \cdot w}{h + w}$$

and according to (6)

$$\frac{a^2}{h + w} = v,$$

so that

$$d^2 = v \cdot w, \tag{7}$$

[4] Lambert, quoted above.

consequently

$$a^2 - d^2 = v(h + w) - v \cdot w = v \cdot h = g^2, \tag{8}$$

so that from (6) and (8)

$$h + w = H = \frac{a^2 \cdot h}{g^2} \tag{9}$$

and finally

$$E_{P-H} = \frac{a^2 \cdot g^4 \cdot B'}{a^2 \cdot g^4 + a^4 \cdot h^2} = \frac{g^4 \cdot B'}{g^4 + a^2 \cdot h^2} \cdot \tag{10}$$

Thus using equation (10) one may determine the horizontal illumination at any point in space in a simple manner, without additional charts or tables, except a polar coördinate paper.

The procedure will be as follows: Determine d from equation

$$d = \tfrac{1}{2}(p_1 - p_2) \tag{11}$$

and make $OC = d$; then make $CK = g$ which is readily done without compass or ruler, by using "Fluxolitepaper." [5]

To illustrate this by a practical example, assume the luminous disc has a radius of $a = 2'$ and a flux density of 100 foot Lambert $= B'$; the height of suspension be $h = 8'$ above working plane and the distance of point P from foot of center is $b = 4'$. Then $p_1 = 10'$ and $p_2 = 8.25'$, so that according to (11) $d = .875'$ and $g = 1.8'$ and

$$E_{P-H} = .039 \cdot 100 = 3.9 \text{ footcandles.}$$

The curves G have thus been established as hyperbolæ and a simple graphical determination of the horizontal illumination at any point in space has been the result.

While thus the flux coming from a luminous disc may be figured as "streamlined" along a system of confocal hyperbolæ rotating around the vertical axis through the disc, Hyde has further shown [6] that for an infinitely long luminous strip a family of confocal ellipses having the same foci as the hyperbolæ are orthogonal to the hyperbolæ and it stands

[5] Highbie, "Lighting Calculations;" 1934, Page 79. Fluxolite paper is a polar coördinate paper upon which a rectangular has been superimposed; it is obtainable at Keuffel & Esser Co., Hoboken, N. J.

[6] *Bulletin of Bureau of Standards*, Vol. 3, No. 1, Reprint No. 51, Page 94.

to reason that the same applies to the luminous disc for which on account of symmetry any vertical cross section through its axis shows the identical condition.

Thus for any point in space, tangents to the hyperbolæ indicate the maximum flux density (illumination vector or even perhaps luminous intensity [7]), the tangents to the ellipses or the planes normal to the hyperbolæ receive the maximum illumination at this point. In other words, the confocal ellipses or rather the oblate spheroids, represented by the ellipses (Fig. 5), form the locus for the maximum illumination

FIG. 5.

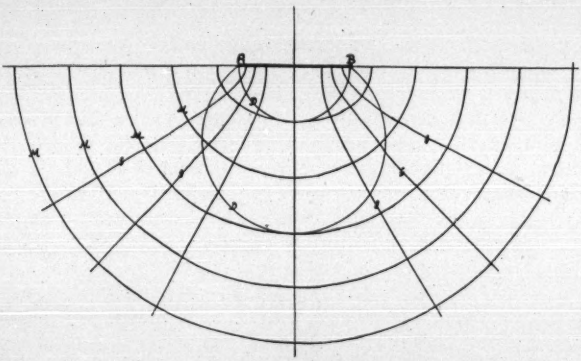

System of confocal hyperbolæ and ellipses for luminous disc.

(illumination) vector and correspond to the concentric spheres (circles C in Fig. 1) of the luminous sphere.

Ellipses have the characteristic that for every point thereof the sum of the distances to the foci is constant. Thus for all cross sections through disc and oblate spheroids, hence also in the plane of the paper of Fig. 4 and Fig. 5 the sum of the distances to the foci A and B is constant and if

$$e = \tfrac{1}{2}(p_1 + p_2), \qquad (12)$$

the average distant of any point in space to the edge of the

[7] Gershun-Moon, "The Light Field," Page 119.

disc (foci A and B), the latter is constant for one and the same ellipse, and e corresponds to the constant distant from the center of a luminous sphere.

The ellipses however do not describe surfaces of constant illumination as in the case of the concentric spheres, but the illumination (illumination vector) decreases from a maximum value on the vertical axis through the disc down to zero in the plane of the disc. The variations follow the course of the ellipse in a definite constant ratio and this leads to an equation like the following:

$$\frac{D^2}{E_0^2} = \frac{e^2 - b^2}{e^2 - d^2}, \tag{13}$$

$$D = E_0 \sqrt{\frac{e^2 - b^2}{e^2 - d^2}}, \tag{14}$$

where D = flux density normal to ellipse at a certain point, E_0 = flux density on center axis of disc on same ellipse, if further Θ = the angle between the direction of D and E_0, it will be shown that

$$\cos \Theta = \sqrt{\frac{e^2 - b^2}{e^2 - d^2}}$$

or that

$$D = E_0 \cdot \cos \Theta \tag{15}$$

and also

$$D = \frac{I_0}{e^2} \cos \Theta, \tag{16}$$

where I_0 = the luminous intensity measured in candle power at right angles to the luminous disc evaluated in the customary way, as

$$I_0 = a^2 \cdot B' = \pi a^2 \cdot B, \tag{17}$$

B' and B being the usual values for brightness.

Now these equations (15) and (16) are of paramount interest, because they are similar in form to the well known (inverse square) formula for normal illumination due to a luminous disc if the latter is taken as point source while in equations (15) and (16) the dimensions of the disc are taken into account and there is no assumption nor approxi-

mation. Naturally the factors used have a different interpretation. In the old approximate formula (17)

$$E_N = \frac{I_0 \cdot \cos \alpha}{r^2}, \tag{17}$$

r = the distance between the disc center and the point of illumination, α = the angle between r and the vertical axis of the disc, while in equation (15) and (16) Θ = the angle between tangent to hyperbola at the point and the vertical axis and in equation (16) e is, as already stated, the average distance between the point of illumination and the edge of the disc, and is constant for a particular ellipse.

For every point in space, there is one Equilux sphere, one hyperbola and one ellipse determining the flux densities due to the luminous disc. The equilux sphere indicates constant flux density normal to its outline as well as the so-called horizontal illumination for a horizontal disc. This flux density or illumination, it may be again called E_H, is thus the same for the point of illumination as for a point T on the equilux sphere vertically below the center of the disc. Its value is thus obtained, as well known from

$$E_H = \frac{a^2 \cdot B'}{a^2 + H^2}. \tag{5}$$

It has not the same value as E_0, which is on the ellipse on a point S below the center of the disc. It has been shown [8] that

$$D = \frac{E_H}{\cos \Theta}, \tag{18}$$

which according to (15) is supposed to be $D = E_0 \cdot \cos \Theta$, so that it would be

$$E_H = E_0 \cdot \cos^2 \Theta. \tag{19}$$

Thus it has to be shown that $E_H/E_0 \cos^2 \Theta$ is equal as per equation (19) as well as equal equation (13).

From simple geometrical relations there is no doubt that in Fig. 4

$$\cos \Theta = \frac{b}{\sqrt{b^2 + w^2}}, \tag{20}$$

[8] Yamauti, quoted above.

thus the proof of equations (15) and (16) is furnished, if it is proven that

$$\cos^2 \Theta = \frac{b^2}{b^2 + w^2} = \frac{e^2 - b^2}{e^2 - d^2} = \frac{e^2}{a^2 + H^2}.$$

For simplicity it seems advantageous to group the various relations systematically by way of tabulation as follows:

$$p_1 = h^2 + (a + b)^2, \tag{21}$$

$$p_2 = h^2 + (a - b)^2, \tag{22}$$

$$e = \tfrac{1}{2}(p_1 + p_2), \tag{23}$$

$$d = \tfrac{1}{2}(p_1 - p_2), \tag{24}$$

$$p_1^2 - p_2^2 = (p_1 + p_2) \cdot (p_1 - p_2) = 4 \cdot a \cdot b, \tag{25}$$

$$a \cdot b = e \cdot d, \tag{26}$$

$$a^2 = v \cdot (h + w), \tag{6}$$

$$b^2 = w \cdot (h + v), \tag{27}$$

$$R^2 = b^2 + (h - \sqrt{R^2 - a^2})^2, \tag{28}$$

$$p^2 \cdot p^2 = [(a + b)^2 + h^2)] \cdot [(b - a)^2 + h^2)], \tag{29}$$

$$R^2 = \frac{p_1^2 \cdot p_2^2}{4 \cdot h^2}, \tag{30}$$

$$p_1 \cdot p_2 = 2 \cdot R \cdot h, \tag{31}$$

$$a^2 + H^2 = 2 \cdot R \cdot H, \tag{32}$$

$$p_1^2 + p_2^2 = 2 \cdot (a^2 + b^2 + h^2), \tag{33}$$

$$v \cdot w = d^2 = \tfrac{1}{4}(p_1 - p_2)^2, \tag{7}$$

$$\frac{h + v}{v} = \frac{b^2}{d^2} = \frac{e^2}{a^2}, \tag{34}$$

$$\frac{h + w}{w} = \frac{a^2}{d^2} = \frac{e^2}{b^2}, \tag{35}$$

$$e^2 = (h + v) \cdot (h + w), \tag{36}$$

$$v = \frac{a^2 - d^2}{h}, \tag{8}$$

$$w = \frac{d^2 \cdot h}{a^2 - d^2} = \frac{b^2 \cdot h}{e^2 - b^2}, \tag{37}$$

$$H = h + w = \frac{a^2 \cdot h}{a^2 - d^2} = \frac{e^2 \cdot h}{e^2 - b^2}, \tag{9}$$

$$h \cdot w = b^2 - d^2, \tag{38}$$

$$w^2 = \frac{b^2 \cdot h \cdot w}{e^2 - b^2} = \frac{b^2 \cdot (b^2 - d^2)}{e^2 - b^2}. \tag{39}$$

Now if equation (39) is used in equation (20), it leads eventually to

$$\cos^2 \Theta = \frac{e^2 - b^2}{e^2 - d^2}.$$

This establishes the correctness of the assumption that the fraction in equation (13) and (14) equals the cosine of the angle Θ between the vertical axis through the disc and the normal to the ellipse at any point P. That the same satisfies also the conditions existing in the equilux sphere as expressed in equations (18) and (19) will be substantiated by showing that

$$\cos^2 \Theta = \frac{b^2}{b^2 + w^2} = \frac{e^2}{a^2 + H^2}.$$

According to equation (32)

$$a^2 + H^2 = 2 \cdot R \cdot H = (H + v + w) \cdot (h + w).$$

According to (36), (38) and (39)

$$a^2 + H^2 = e^2 + \frac{e^2 \cdot w^2}{b^2} = \frac{e^2}{b^2}(b^2 + w^2), \tag{40}$$

which proves the above contention.

It thus has been demonstrated at least for the luminous disc that the so called illumination vector D may be calculated by means of a inverse square equation with absolute correctness and without approximation, if instead of the distance from center disc the average distance from the edge of the disc is used and if the cosine law of emission is related to the cosine of that angle which the true direction of the illumination vector forms again with the vertical axis of the disc.

This true direction of the illumination vector is normal to the ellipse which is the cross section through an oblate spheroid and which is determined by the edge-points of the disc in cross section as foci.

The luminous intensity causing this illumination vector assumes thus an actual physical condition as the force which is the integral of all contributions from the luminous particles of the disc to the flux density at this point and has the direction normal to the ellipse or tangent to the hyperbola having the nearest edge point of the disc as focus.

It remains to illustrate these relations by a practical example which shall be done by choosing the same relations as accepted above: there is thus

$$I_0 = a^2 \cdot B' = 400 \text{ candle power},$$
$$e = \tfrac{1}{2}(p_1 + p_2) = 9.125,$$
$$e^2 = 83.2656,$$
$$\cos \Theta = \sqrt{\frac{e^2 - b^2}{e^2 - d^2}} = \sqrt{\frac{83.27 - 16}{83.27 - .77}} = .9045.$$

Therefore

$$D = \frac{I_0}{e^2} \cos \Theta = \frac{400}{83.27} .9045 = 4.35 \text{ footcandles.}$$

This is thus the maximum or normal illumination at the selected point in a plane inclined by an angle of 25°15′ against the horizontal and caused by an intensity of 361.8 *cp* in a direction of 25°15′ against the vertical. The horizontal illumination at the point is

$$E_H = D \cdot \cos \Theta = 4.35 \cdot .9045 = 3.9 \text{ footcandles,}$$

which must be the same value as obtained above by means of equation (10), while the illumination in a vertical plane

$$E_V = D \cdot \sin \Theta = 4.35 \cdot .4266 = 1.86 \text{ footcandles.}$$

ON THE STABILITY AND MAGNITUDE OF ELECTRONIC CHARGES. PART II, SCALAR WAVE FUNCTIONS.

BY

ALFRED LANDÉ and LLEWELLYN H. THOMAS,*

Mendenhall Laboratory, Ohio State University.

1. INTRODUCTION.

The question of how electronic particles can exist in space and time under the laws of relativity and quantum theory splits up in two separate problems. First, if the particle is supposed to be characterized by a fundamental momentum (mc) and a fundamental length a reciprocal to m, then how large is the product amc (which is independent of m)? The answer has been found [1] in Part I. The numerical ratio $amc/\hbar$ in the most stable ground state is

$$\mu = amc/\hbar = 0.02985037\ldots$$

as the smallest solution of the transcendental equation $2\pi\mu[Y_0(\mu)]^2 = 1$. See also this Part II section 4.

The second question is that of how large is the length a? Or, if a is written in the form $a = \gamma e^2/mc^2$, how large is the numerical factor γ? If γ were known we would be able to predict the value of Sommerfeld's fine structure constant

$$\alpha = e^2/c\hbar = \gamma^{-1}(\gamma e^2/mc^2)mc\cdot\hbar^{-1} = \mu/\gamma.$$

Although we do not have a unique way of calculating γ, certain physical considerations (see below) seem to leave only *two* reasonable choices for γ. The one is $\gamma = 4\cdot(2/3)^{1/2}$ obtained when a is the *diameter* of J. J. Thomson's cross-section σ of a free electric particle scattering infrared light, $\sigma = (8\pi/3)(e^2/mc^2)^2$ so that $(a/2)^2\pi = \sigma$ with a *circular* area σ. The other choice of γ is obtained from the still simpler formula $a^2 = 2\sigma$ so that a is the *diagonal* of a *quadratic* area σ.

* Sections 1–4 by A. L., Section 5 by L. H. Th.

[1] A. Landé, Part I, JOUR. FRANK. INST., 229, 767, 1940.

It is noteworthy that the latter choice

$$a^2 = 2\sigma, \quad \text{that is,} \quad \gamma = 4\cdot(\pi/3)^{1/2} = 4.093307\ldots$$

immediately yields

$$\alpha = \frac{\mu}{\gamma} = \frac{1}{137.1273}.$$

The value of μ was derived a priori, and only the factor 2 in $a^2 = 2\sigma$ has been chosen a posteriori. The physical reason why (a/c) should be the time for a light signal to travel across σ will be discussed in a separate paper.

Our way of arriving at the proper values of μ is related to the theory of Born and Fuchs [2] but differs in the method as well as in the results.

2. THE INTEGRAL EQUATION.

We are using reduced coördinates and momenta

$$R = r/a, \quad T = ct/a, \quad P = p/mc, \quad E = \epsilon/mc^2. \tag{1}$$

Einstein's and the signal equation then read

$$E = \pm (P^2 + 1)^{1/2}, \tag{2}$$

$$T = \pm (R^2 + 1)^{1/2}. \tag{2'}$$

In Part I we wrote Δr and Δt instead of r and t in order to emphasize the interval character of r and t. Through (2) (2') the wave functions $\psi(\boldsymbol{R}, T)$ and $\chi(\boldsymbol{P}, E)$ become functions of the vectors $\boldsymbol{R}$ and $\boldsymbol{P}$ alone and of the *sign* of T and E:

$$\psi_+(\boldsymbol{R}), \quad \psi_-(\boldsymbol{R}), \quad \chi_+(\boldsymbol{P}), \quad \chi_-(\boldsymbol{P}).$$

The ground solution of the Schrödinger-Klein-Gordon equation for a free particle is an exponential function

$$\exp\left[i\hbar^{-1}(\boldsymbol{p}\cdot\boldsymbol{r} + \epsilon t)\right].$$

We may build up more general solutions in the form of Fourier integrals

$$\psi(\boldsymbol{R}) = (\mu/2\pi)^{3/2}\int\chi(\boldsymbol{P})\exp\left[i\mu(\boldsymbol{P}\cdot\boldsymbol{R} + ET)\right]dW_0, \tag{3}$$

$$\chi(\boldsymbol{P}) = (\mu/2\pi)^{3/2}\int\psi(\boldsymbol{R})\exp\left[-i\mu(\boldsymbol{P}\cdot\boldsymbol{R} + ET)\right]dV_0. \tag{3'}$$

[2] M. Born, *Proc. Roy. Soc. Edinburgh*, **59**, 219, 1939. Born and Fuchs, ibid., **60**, 100 and 141, 1940.

dW_0 and dV_0 are the invariant volume elements on the hyperboloids (2) (2′)

$$\begin{aligned} dW_0 &= P^2 dP d\phi d(\cos\theta)\,|E|^{-1}, \\ dV_0 &= R^2 dR d\varphi d(\cos\vartheta)\,|T|^{-1}, \end{aligned} \tag{4}$$

whereas μ is an abbreviation for the positive numerical factor

$$\mu = amc/h (= \gamma \cdot \alpha, \text{ see introduction}). \tag{4′}$$

The integrations in (3) (3′) shall be carried over positive and negative values of E and T respectively. The factor $(\mu/2\pi)^{3/2}$ is chosen so that (3′) would be the direct inversion of (3) were it not for the factor $\exp(i\mu ET)$ and the relativistic denominators $|E|^{-1}$ and $|T|^{-1}$ in dW_0 and dV_0. That is, the nonrelativistic approximation of (3) (3′) could be solved for every function ψ and for every value of μ. In fact, however, (3) (3′) are satisfied by certain selected proper functions ψ and proper values μ only.[3] When solving (3) (3)′ we may consider two special cases:

$$\psi_- = \psi_+, \qquad \chi_- = \chi_+, \tag{a}$$

or

$$\psi_- = -\psi_+, \qquad \chi_- = -\chi_+, \tag{b}$$

so that ψ_+ and χ_+ satisfy the equations obtained from (3) (3′)

$$\psi_+(\boldsymbol{R}) = (\mu/2\pi)^{3/2} 2 \int \chi_+(\boldsymbol{P}) \times \exp(i\mu \boldsymbol{P}\cdot\boldsymbol{R}) \left\{ \begin{matrix} \cos \\ i \sin \end{matrix} (\mu|E||T|)\cdot dW_0, \quad \left(5 \begin{matrix} a \\ b \end{matrix}\right\}\right)$$

$$\chi_+(\boldsymbol{P}) = (\mu/2\pi)^{3/2} 2 \int \psi_+(\boldsymbol{R}) \times \exp(-i\mu \boldsymbol{P}\cdot\boldsymbol{R}) \left\{ \begin{matrix} \cos \\ -i \sin \end{matrix} (\mu|E||T|)\cdot dV_0. \quad \left(5' \begin{matrix} a \\ b \end{matrix}\right\}\right)$$

When ψ_+ and χ_+ have been found then ψ_- and χ_- are defined by (a) (b). In Part I we considered wave functions of spherical symmetry ($l = 0$). Here we discuss angular wave functions ($l = 0, 1, 2, \cdots$) in general.

[3] A proper value problem of a similar kind was first suggested in JOUR. FRANK. INST., 228, 459, 1939. M. Born (Part I) first suggested an integral equation not very different from (3) (3′).

3. ANGULAR WAVE FUNCTIONS. INTEGRAL EQUATION.

If ψ and χ depend on ϑ, φ and θ, ϕ respectively we factorize

$$\begin{aligned}\psi(\boldsymbol{R}) &= \psi(R)\mathfrak{P}_l^m(\cos\vartheta)\exp(im\varphi),\\ \chi(\boldsymbol{P}) &= \chi(P)\mathfrak{P}_l^m(\cos\theta)\exp(-im\phi).\end{aligned}\tag{6}$$

The angular factors (spherical harmonics) shall be normalized to unity. We then have the expansion

$$\begin{aligned}\exp(i\mu\boldsymbol{P}\cdot\boldsymbol{R}) &= \exp\big[i\mu PR(\cos\vartheta\cos\theta+\sin\vartheta\sin\theta\cos(\varphi-\phi))\big]\\ &= \sum_0^\infty i^l\sum_0^l m(2\pi)^{3/2}i^l(\mu PR)^{-1/2}J_{l+\frac12}(\mu PR)\\ &\quad\times\mathfrak{P}_l^m(\cos\vartheta)\mathfrak{P}_l^m(\cos\theta)\cdot\cos\big[m(\varphi-\phi)\big].\end{aligned}$$

This and (6) substituted in (5) (5′) leads to the equations

$$\psi_+(R) = i^l\mu^{3/2}2\int_0^\infty \chi_+(P)\times\frac{J_{l+\frac12}(\mu PR)}{(\mu PR)^{1/2}}\left\{\begin{matrix}\cos\\ i\sin\end{matrix}(\mu|T||E|)P^2dP_0,\quad\left(7\begin{matrix}a\\ b\end{matrix}\right)\right\}$$

$$\chi_+(P) = (-i)^l\mu^{3/2}2\int_0^\infty \psi_+(R)\times\frac{J_{l+\frac12}(\mu PR)}{(\mu PR)^{1/2}}\left\{\begin{matrix}\cos\\ -i\sin\end{matrix}(\mu|T||E|)R^2dR_0\quad\left(7'\begin{matrix}a\\ b\end{matrix}\right)\right\}$$

if we use the abbreviations

$$\begin{aligned}R &= \sinh R_0, & |T| &= \cosh R_0, & |T|^{-1}dR &= dR_0,\\ P &= \sinh P_0, & |E| &= \cosh P_0, & |E|^{-1}dP &= dP_0.\end{aligned}\tag{8}$$

The two interlocked equations (7) (7′) for ψ and χ can be reduced to one equation for ψ and another equation of the same form for χ if we consider the particular cases

either $$\psi(x) = (\pm)i^l\chi(x),\tag{A}$$

or $$\psi(x) = (\pm)i^{l+1}\chi(x).\tag{B}$$

Born's "reciprocity" appears to be a particular way (A) of solving the quantum problem (3) (3′). The case (B) however turns out to be more important.

A real symmetric kernel is obtained in the two combination

cases (Aa) and (Bb) where (7) (7′) reduce to the final integral equation

$$\psi_+(R) = (\pm)\mu^{3/2}2\int_0^\infty \psi_+(P) \times \frac{J_{l+\frac{1}{2}}(\mu PR)}{(\mu PR)^{1/2}} \left\{ \begin{matrix} \cos \\ \sin \end{matrix} (\mu|T||E|)P^2 dP_0 \quad \left(9 \begin{matrix} Aa \\ Bb \end{matrix} \right\} \right)$$

and the same equation for χ. The remaining task is that of solving equation (9) for $l = 0, 1, 2 \cdots$.

An abbreviated way of obtaining (7) (7′) and then (9) is this. Substitute the product (6) into the wave equation for $\psi(R)$

$$\nabla^2\psi - \partial^2\psi/\partial T^2 = \mu^2\psi.$$

This leaves for $\psi(R)$ the equation

$$\frac{1}{R^2}\frac{d}{dR}\left(R^2\frac{d\psi}{dR}\right) - \frac{l(l+1)}{R^2}\psi(R) = -\mu^2(E^2-1)\psi(R), \quad (10)$$

which is solved with $E^2 - 1 = P^2$ by

$$\psi(R) = \text{const.}\ (\mu PR)^{-1/2}J_{l+\frac{1}{2}}(\mu PR).$$

Supplying this ground solution with the relativistic factor $\exp(i\mu ET)$ and with an amplitude $\mu^{3/2}i^l\chi(P)$ and integrating over dW_0 one arrives at (7). Since the angular momentum and its z-component are functions symmetric in r and p, the state (l, m) can also be described in momentum space which leads to (7′). The factor $\mu^{3/2}$ in front is chosen so that (7′) is the inversion of (7) in the nonrelativistic limit according to the Fourier-Bessel formula

$$G(\xi) = \int_0^\infty F(\eta)J_s(\xi\eta)\eta d\eta, \qquad F(\eta) = \int_0^\infty G(\xi)J_s(\xi\eta)\xi d\xi.$$

4. SOLUTION OF THE INTEGRAL EQUATION FOR $l = 0$.

For $l = 0$ the Bessel function $J_{l+\frac{1}{2}}$ reduces to

$$J_{\frac{1}{2}}(z) = (2/\pi)^{1/2}z^{-1/2}\sin(z),$$

so that instead of (9) we have to solve the integral equation

$$[R\cdot\psi(R)] = (\pm)(2\mu/\pi)^{1/2}2\int_0^\infty [P\cdot\psi(P)] \times \sin(\mu PR)\begin{Bmatrix}\cos\\ \sin\end{Bmatrix}(\mu|T||E|)dP_0. \quad \left(11\begin{matrix}aA\\ bB\end{matrix}\right)$$

With the help of (8) we have shown in Part I that the solution is

$$\psi_\nu(R) = \sin(\nu R_0)\cdot R^{-1} = \sin(\nu R_0)\cdot(\sinh R_0)^{-1} \qquad (12)$$

for continuous values of the parameter ν. The proper value μ thereby has to satisfy the equation

$$1 = (\pm)\sqrt{2\pi\mu}\,\frac{2}{\pi}\int_0^\infty \begin{matrix}-\sin\\ \cos\end{matrix}(\mu\cosh x)\cos(\nu x)dx, \quad \left(12'\begin{matrix}Aa\\ Bb\end{matrix}\right)$$

correcting a typographical error in (23) Part I. The smallest proper value is obtained in the limit $\nu = 0$ where (12′) reads

$$1 = (\mp)\sqrt{2\pi\mu}\begin{Bmatrix}J_0(\mu)\\ Y_0(\mu)\end{Bmatrix} \qquad \left(12''\begin{matrix}Aa\\ Bb\end{matrix}\right)$$

with the smallest solutions $\mu = \begin{cases}0.157\\ 0.0299\end{cases}$ respectively. The corresponding proper function in both cases is

$$\psi_0 = \text{const.}\ R_0R^{-1} = \text{const.}\ R_0\cdot(\sinh R_0)^{-1}.$$

Proper functions $\psi_\nu(R)$ of (12) belonging to different parameters ν are mutually orthogonal and normalized to unity in so far as they satisfy the equation

$$\lim_{A=\infty}\frac{1}{A}\,2\int_0^A \psi_\nu\psi_{\nu'}R^2dR_0 = \delta_{\nu\nu'}. \qquad (13)$$

($4\pi R^2dR_0$ is the invariant volume element). This is true also in the limit $\nu \approx 0$ where $\psi \approx (\nu R_0)\cdot R^{-1}$. The physical significance of the smallest proper value $\mu = 0.0299$ was discussed in the introduction.

Other solutions of (11) are the functions [replace ν by $i\kappa$ in (12) (12′)!]

$$\psi_\kappa(R) = \sinh(\kappa R_0)\cdot R^{-1} = \sinh(\kappa R_0)\cdot(\sinh R_0)^{-1} \qquad (14)$$

for proper values μ determined by the transcendental equation

$$1 = (\pm)\sqrt{2\pi\mu}\,\frac{2}{\pi}\int_0^\infty \begin{matrix}-\\ \cos\end{matrix}\ (\mu\cosh x)\cosh(\kappa x)dx. \qquad \left(14'\ \begin{matrix}Aa\\ Bb\end{matrix}\right)$$

For $|\kappa| > 1$ (14) is infinite at $R = \infty$ and does not represent a proper function. For $|\kappa| < 1$ (14) vanishes at $R = \infty$, but is not integrable in the sense of (13). Therefore the proper values μ of (14'), always larger than 0.0299, do not have a physical significance.

5. SOLUTION FOR EVERY l.

In order to solve the integral equation (9) for every $l = 0, 1, 2 \cdots$ we refer to a mathematical theorem (similar to a theorem of Gegenbauer, see Watson, Bessel functions, 1922, p. 379).

The integral equation

$$2\int_0^\infty \psi(P)(\mu\sinh R_0\sinh P_0)^{-1/2}J_{l+\frac{1}{2}}(\mu\sinh R_0\sinh P_0) \times \exp(i\mu\cosh R_0\cosh P_0)\sinh^2 P_0 dP_0 = \frac{1}{\Lambda}\psi(R) \qquad (15)$$

is solved by the proper functions[4]

$$\psi_{\kappa,l}(R) = \sinh^l R_0\left(\frac{d}{d\cosh R_0}\right)^l \frac{\sinh(\kappa R_0)}{\sinh R_0} \qquad (16)$$

for proper values

$$\frac{1}{\Lambda_{\kappa,l}} = i^{l+1}\sqrt{2\pi}\mu^{-1}\,\frac{2}{\pi}\int_0^\infty \exp(i\mu\cosh x)\cosh(\kappa x)dx \qquad (16')$$

and continuous values of κ. $\psi_{l,\kappa}$ vanishes at infinity if κ is either real between -1 and $+1$, or purely imaginary $\kappa = i\nu$ with ν between $-\infty$ and $+\infty$. $\psi_{l,\kappa}$ in (16) then is either real or purely imaginary, too. We therefore may split (15) in its real and imaginary parts and arrive at two separate cases:

[4] It can at once be verified by differentiating the equation (15) that its solutions satisfy the differential equation

$$\frac{1}{R^2}\frac{d}{dR_0}\left(R^2\frac{d\psi}{dR_0}\right) - \frac{l(l+1)}{R^2}\psi(R) = -\mu^2\psi(R),$$

which is a modification of (10).

If l is *odd* then i^{l+1} is real, and (9 *Aa*) resp. (9 *Bb*) is solved by the proper function (16) whereby μ is determined by the transcendental equation

$$1 = (\pm) i^{l+1} \sqrt{2\pi\mu}\, \frac{2}{\pi} \int_0^\infty \begin{matrix}\cos \\ \sin\end{matrix} (\mu \cosh x) \cosh (\kappa x) dx. \quad (17)$$

If l is *even* then i^{l+1} is imaginary, and (9) is solved by the proper function (16) whereby μ is determined by

$$1 = (\pm) i^{l} \sqrt{2\pi\mu}\, \frac{2}{\pi} \int_0^\infty \begin{matrix}-\sin \\ \cos\end{matrix} (\mu \cosh x) \cosh (\kappa x) dx. \quad (18)$$

If κ is purely imaginary, $\kappa = i\nu$, $\sinh (\kappa R_0) = i \sin (\nu R_0)$, $\cosh (\kappa x) = \cos (\nu x)$, then (16) represents an integrable proper function in the sense of (13). If κ is real between -1 and $+1$ then $\psi_{\kappa,l}$ still vanishes at infinity but is not integrable any more. When comparing (17) (18) with (12′) one learns that the proper value spectra for every l are the same as for $l = 0$ except for the various *cases* (*Aa*), (±) etc. in which they occur. Our proper functions and proper value spectra are quite different from those obtained by Born and Fuchs l.c. The most significant result of the quantization is the smallness of the proper value $\mu \sim 0.03$. This together with the largeness of the Thomson cross-section ($\gamma \sim 4.1$) leads to the small value of $\alpha = \mu/\gamma$. The result rests on the signal equation which had been proposed as an example of Born's idea of *reciprocity*.

NOTES FROM THE NATIONAL BUREAU OF STANDARDS.*

REVISED STANDARD FREQUENCY BROADCASTS.

The Bureau's standard frequency station, WWV, was destroyed by fire November 6. A temporary transmitter has been established in another building and has begun a reduced service. It broadcasts the frequency five megacycles (=5000 kilocycles) per second, every day (except Sunday) from 10 A.M. to midnight. This is continuous-wave only, with telegraphic code announcements of the call letters WWV every 20 minutes. The accuracy of the frequency is the same as in the past, viz., better than a part in ten-million.

The broadcast is from a 1-kilowatt transmitter. Generally speaking, it is most useful for moderate distances in the daytime and long distances at night. More precisely, for reception in locations reasonably free from interference, it is receivable at all distances up to 1000 miles from Washington in the middle of the day. The distance range increases after about 4 P.M. (E.S.T.) until at night the broadcast is receivable throughout the United States; sometimes at night it may be difficult to receive it at distances between 50 and 500 miles, while it is easy to receive it beyond 500 miles. In the spring the daytime distance range will decrease, dropping to about 500 miles in the summer.

This restricted service will continue for some months. As rapidly as possible a new station will be established to provide more fully than in the past, standard frequencies receivable at all times throughout the country. These will include standard radio frequencies, standard seconds pulses, and the standard of musical pitch, 440 cycles per second, which will unfortunately not be available during the period in which the temporary transmitter is used.

* Communicated by the Director.

ALTERNATING CURRENT GROUNDS ON WATER PIPES.

The technical subcommittee of the American Research Committee on Grounding has been investigating complaints covering damage to water systems in houses and pollution of water flowing in the pipes. The Bureau is represented in this work by Morton G. Lloyd, Chief of the Safety Codes Section.

The subcommittee has issued a summary report covering 21 complaints in 7 communities, showing that in none of these cases was there evidence to indicate that the flow of alternating current over water pipes or mains by itself has caused damage to the piping or to the water flowing in the pipes. On the other hand, the investigations revealed differences in the chemical composition of the water supplied to a given user; differences in impurities of the metal of which the pipes are made; galvanic action resulting from the indiscriminate use of many different metals, and variations in their composition; differences in the temperature of the hot water supply, and in the rate and amount of water drawn from the mains; and many other factors.

It has not been possible to develop thoroughly all of the complex variables present in the different situations investigated, and definite conclusions are rendered more difficult because of the inability of the subcommittee to obtain more cases for investigation. It is, therefore, not possible at this time to state that damage from alternating current flowing over water pipes could not occur.

For the future, the Grounding Committee expects to continue its investigation of all complaints of water contamination where grounding of electrical circuits is involved, to determine, if possible, whether there is any relation in normal practice between superimposed alternating currents and effects on water pipes and the water itself. The Committee also proposes to establish simple test set-ups where accelerated reactions might be obtained if such a relation does exist. These set-ups would be of such a nature as not to require continuous observations; but would be placed in water plants or laboratories where occasional checks could be made under the supervision of skilled personnel. However, the necessity for prompt investigation of all complaints would still exist, so as to gain field experience and to correlate the various factors involved.

PREPARATION OF BENZOIC ACID OF HIGH PURITY.

In the *Journal of Research* for December, Frank W. Schwab and Edward Wichers describe (RP1351) the preparation of benzoic acid of extremely high purity.

For many years benzoic acid has been used as a standard substance in acidimetry and for the calibration of bomb calorimeters. Certified samples of the material have been issued by the Bureau since 1911. Recently, it became necessary to prepare some of the material of the highest practicable purity, primarily for a determination of the heat of combustion of the pure substance.

A number of methods for preparing pure benzoic acid were compared, both with respect to the degree of purity and the ease with which it could be attained. Simultaneously, a study was made of means for determining the purity of the substance. The methods adopted for determining purity were based on very precise determinations of the freezing range of the acid, and on measurements of the specific heat of the solid substance at temperatures closely approaching its melting point.

The methods of preparation which were studied were: Purification of a commercial material, which was about 99.98 per cent. pure by fractional distillation in vacuum; fractional freezing, and crystallization from solvents; and preparation from other substances by selected reactions. A purity of 99.999 mole per cent. was attained by each of three methods: Crystallization from benzene; fractional freezing; and hydrolysis of benzoyl chloride, purified by fractional distillation. Crystallization from water gave material 99.996 per cent. pure in the same number of steps that yielded the purer material by crystallization from benzene. The ready availability of pure water partly offsets the advantage of the more rapid purification from benzene. Hydrolysis of benzoyl chloride is rapid and easy but involves painstaking preliminary purification of the parent substance. Fractional freezing is a relatively simple and rapid method. The freezing point of benzoic acid is tentatively given as 122.36° C. ± 0.01° C.

STANDARD COLOR TEST FOR PORCELAIN ENAMELS.

For several years the Bureau has coöperated with the Porcelain Enamel Institute in developing standard tests for porcelain enamels. One current project is a standard test for evaluating color differences between nearly identical specimens. For this work a special subcommittee of the Institute was formed, members of which prepared 15 sets of 13 specimens each. Every set consisted of a central standard and 12 other specimens having slight, systematic differences from the standard in their hue saturation and lightness. The colors of the central standards were widely varied within the possible range.

Visual estimates of the directions and magnitudes of the differences between the central standards and the similarly colored specimens in the respective sets have been made at the Bureau and at several coöperating laboratories. Additional estimates are planned. Several different means of determining these differences by computation from data obtained on various instruments are also being tried. It is planned to modify the formulas or, if necessary, one or another of the instruments, until reasonably good agreement between such determinations and the averages of visual estimates can be obtained. If this can be done successfully, the instrumental method will be recommended as standard, and can be used both as a control method for manufacturers and a test method for purchase specifications.

SPECIFIC REFRACTION AND DISPERSION OF GLASSES.

Recently John C. Young and A. N. Finn, chief of the Bureau's Glass Section, have made many new glasses of unusual composition, containing, in varying amounts, such elements as rubidium, cesium gallium, yttrium, indium, lanthanum, cerium, praseodymium, neodymium, samarium, gadolinium, holmium, erbium, columbium, tantalum, etc. Refractive index and density data on these glasses, as well as similar data from the literature on the ordinary constituents of glass, have been examined statistically to determine the applicability to glass of several of the better known specific refraction ratios. It was found that of these ratios only the Gladstone-Dale

ratio possesses each of the following features: For any specified wave-length of light it is independent of the thermal history of a given glass, and it varies linearly with composition. It is also useful, in combination with "specific dispersion," for computing the ν-value, or "dispersive index," of a glass.

In RP1352, which will be published in the December number of the *Journal of Research*, definite numerical factors are given for 32 glass-making oxides, from which one can compute the specific refreaction as well as the dispersive index or ν-value of a glass composed entirely of any or all of these oxides. These factors are shown to be related to the periodicity of the elements. The ability to predict the dispersive index (ν) of a glass should be of considerable interest to optical glass manufacturers because it will assist them in designing better glasses for telescopes, binoculars, cameras, etc.

PORE SYSTEM IN BRICKS AND ITS RELATION TO FROST ACTION.

Certain properties associated with the porous structure of bricks have an important bearing on their durability when exposed to the wheather. These properties have received scant attention heretofore and an investigation was made by Ray T. Stull and Paul V. Johnson to obtain data on these properties and on their relation to the failure of bricks as a result of freezing and thawing. Seven series of bricks, the products of five different manufacturers were selected to represent ranges in hardness, methods of manufacture, and temperature at which they had been burned. The properties determined were: Per cent. porosity; variation in porosity within a brick; permeability to air and water; the flow of air through two members in series; effect of time, under continuous flow, on the water permeability; the mean capillary radius and the number of capillaries in an ideal structure which would have the same permeability as that determined experimentally for the brick; saturation coefficient by 48 hours immersion; increase in saturation coefficient with repeated freezing and thawing, and the resistance of bricks to failure by repeated freezing and thawing.

The variation in porosity of a brick is partly responsible for its lack of uniform structure and is, therefore, a con-

tributing factor affecting its life when subjected to repeated freezing and thawing.

No definite correlation was found as to location of lowest, medium, and highest porosities of individuals among the bricks tested. The differences between maximum and minimum per cent. porosities of the different sections of the individual bricks ranged from 2.8 to 10.4, a spread of 11.6 to 48.4 per cent.

When the air permeability values f_1 and f_2 of two members composing a unit, and their relative thicknesses T_1 and T_2 are known, the air conductance, F, of the unit can be determined by application of the equation

$$F = \frac{f_1 f_2}{f_1 T_2 + f_2 T_1}.$$

The differences between the calculated and experimental F values determined were so small as to be negligible.

The mean effective capillary radius, permeability, and number of cycles of freezing and thawing to cause failure of the bricks increase, and the pore volume, number of capillaries, and saturation coefficient decrease with increase in burning temperature. The decrease in pore volume and number of pores indicates that some pores have become filled or sealed and, therefore, inactive so far as permeability and absorption are concerned. The increase in mean effective capillary radius and decrease in number of capillaries indicate that the pores rendered inactive were chiefly the smaller ones originally occurring as micro-cavities formed by the micro-particles.

The air permeabilities were constant with respect to time of flow, whereas the water permeabilities varied, increasing with time for those bricks having mean capillary radii less than 2 microns and decreasing for those with radii greater than 2 microns.

The saturation coefficient increases with increase in the number of freezing and thawing cycles. The relation between these two variables appears to be hyperbolic in character, and may be expressed empirically by the equation:

$$S = a - \frac{K}{b + C},$$

where S is saturation coefficient, C, the cycles of freezing and thawing, and a, b and K are constants for a definite brick but different for different bricks. The constant a represents (theoretically) the upper limiting value of the saturation coefficient under the assumption that the brick would stand an infinite number of freezing and thawing cycles.

Bricks considerably laminated may attain saturation coefficients greater than unity by repeated freezing and thawing, thus containing larger volumes of water than their initial pore volumes.

The general trend of the data indicates that the number of cycles of freezing and thawing to cause failure of the brick increases when the permeability and effective capillary radius increase, and when the porosity, number of capillaries, and saturation coefficient decrease.

The Journal of Research for December will contain the complete account of this investigation, which will be published as RP1349.

Butyl Rubber.—R. M. THOMAS, I. E. LIGHTBOWN, W. J. SPARKS, P. K. FROLICH AND E. V. MURPHREE, writing in *Industrial and Engineering Chemistry*, Vol. 32, No. 10, present the results of a thoroughly unorthodox approach to the synthetic rubber problem. In developing their new butyl rubber, the Esso Laboratories have turned to simple olefins rather than diolefins or more complicated chemical derivatives as the main raw material. Not only is this an economic advantage, but the ready availability of such simple olefins from refinery cracking operations makes the process seem attractive from the standpoint of potential supply of synthetic rubber. As only the limited amount of unsaturation required for curing with sulfur has been provided, the vulcanizates are substantially saturated and therefore possess the chemical stability characteristic of a paraffin hydrocarbon. In spite of this radical difference in internal structure, the polymer can be processed in much the same manner as natural rubber, and the physical properties of natural rubber have been retained to a surprising extent. Because of the low degree of unsaturation and consequent chemical inertness, the available information indicates that butyl rubber will be superior to natural rubber for many purposes.

R. H. O.

THE FRANKLIN INSTITUTE.

STATED MONTHLY MEETING, DECEMBER 18, 1940

The regular monthly meeting of The Franklin Institute was called to order at 8:15 o'clock, by Dr. Henry Butler Allen, Secretary and Director.

The minutes of the November meeting were approved as printed in the December issue of the Journal.

The presiding officer then introduced Dr. John D. Mahoney who gave a short talk on the United Charities Drive in Philadelphia and asked for coöperation of the members of the Institute.

Dr. Allen then announced, with profound sorrow, the great loss suffered by The Franklin Institute in the death of Mr. Alfred Rigling, for fifty-eight years Librarian, and Assistant Secretary and Assistant Editor since 1908. He stated that the Resolution adopted by the Board of Managers would appear in the next issue of the Journal.

As Secretary Dr. Allen then stated that this was the regular monthly meeting of the Institute, and gave the following additions to membership since the report of last month:

Active	12
Associate	7
Student	15
Total	34

In accordance with Article IV, Section 4, of the By-Laws, which states that nominations should be made in writing at this meeting, he then read the following nominations for Officers and Managers for the term beginning January, 1941, giving the names of the sponsors:

President

(to serve one year).
Philip C. Staples

Vice-Presidents

(to serve one year).
Walton Forstall
W. Chattin Wetherill
S. S. Fels
Richard W. Lloyd

Treasurer

(to serve one year).
M. M. Price

Members of the Board of Managers

(to serve three years).
G. H. Clamer
Clarence L. Jordan
Leonard H. Kinnard
Conrad N. Lauer
Lionel F. Levy
Richard T. Nalle
Charles Penrose
Philip H. Ward, Jr.

(to serve two years).
Edward Warwick

(to serve one year).
Charles S. Redding

Dr. Allen then introduced Dr. Alexander Silverman, Professor of Chemistry, University of Pittsburgh, who addressed the meeting on "Glass: Today and Tomorrow."

The speaker described the history of glass making, present manufacturing methods, mirrors, case hardening glass, stresses and strains, glass cloth, and the art side of the industry.

His lecture was profusely illustrated both with lantern slides and experiments. A room with furniture and hangings all made of glass, recently displayed at the World's Fair in New York, was set up in the lecture hall, while a beautiful evening gown made of glass was displayed by a living model.

The meeting was adjourned with a rising vote of thanks to the lecturer, after which the audience spent some time in examining the interesting exhibits.

HENRY BUTLER ALLEN,
Secretary.

LIBRARY NOTES.

The committee on Library desires to add to the collections of the Institute any technical writings of members who have had occasion to publish such material.

Literary contributions from author-members will be gratefully acknowledged, properly inscribed and noted in the Journal of the Institute.

Photostat Service. Photostat prints of any material in the collections can be supplied on request. Orders received in the morning are filled the same day. The average cost for a print $8\frac{1}{2} \times 11$ inches is forty cents.

The library and reading room are open Mondays, Tuesdays, Fridays and Saturdays from nine o'clock A.M. until five o'clock P.M., Wednesdays and Thursdays from two until ten o'clock P.M.

RECENT ADDITIONS.

AERONAUTICS.

DAY, KARL S. Instrument and Radio Flying. 1938.
VETTER, ERNEST G. Aeronautics Simplified. 1940.

ASTRONOMY.

U. S. Hydrographic Office. The Sumner Line of Position. 1930.

BIOGRAPHY.

BRUCE, WILLIAM CABELL. Benjamin Franklin Self-Revealed. Two Volumes. 1917.
CROWTHER, J. G. Men of Science. 1936.

CHEMISTRY AND CHEMICAL TECHNOLOGY.

Chemical Engineering Catalog. Twenty-fifth Annual Edition. 1940.
MARK, H. Physical Chemistry of High Polymeric Systems. 1940. High Polymers. Vol. 2.
PIERCE, WILLIS CONWAY, AND EDWARD LAUTH HAENISCH. Quantitative Analysis. Second Edition. 1940.

SEIDELL, ATHERTON. Solubilities of Inorganic and Metal Organic Compounds. Third Edition. Volume 1. 1940.

WILLARD, HOBART H., AND N. HOWELL FURMAN. Elementary Quantitative Analysis. Third Edition. 1940.

DICTIONARIES.

TWENEY, C. F., AND L. E. C. HUGHES, Editors. Chambers's Technical Dictionary. 1940.

ELECTRICITY AND ELECTRICAL ENGINEERING.

American Radio Relay League. The Radio Amateur's Handbook 1941. 1940.

PARSONS, R. H. The Early Days of the Power Station Industry. 1940.

ENGINEERING.

American Society for Testing Materials. Index to Proceedings, Volumes 31–35 (1931–1935). 1937.

HAYDEN, ARTHUR G. The Rigid-Frame Bridge. Second Edition. 1940.

EXPOSITIONS, MUSEUMS, ETC.

New York Museum of Science and Industry. Exhibition Techniques. 1940.

GEOGRAPHY AND TRAVEL.

RIESENBERG, FELIX. The Pacific Ocean. 1940.

MANUFACTURES.

SPOWERS, WILLIAM H., JR. Hot-Dip Galvanizing Practice. 1938.

MATHEMATICS.

BURINGTON, RICHARD STEVENS. Handbook of Mathematical Tables and Formulas. 1940.

METEOROLOGY.

ELM, IENAR E. Weather and Why. 1929.

MINING AND METALLURGY.

American Institute of Mining and Metallurgical Engineers. Transactions. Metal Mining. 1940.

SACHS, GEORGE, AND KENT R. VAN HORN. Practical Metallurgy. 1940.

NAVAL ARCHITECTURE AND NAVIGATION.

SKENE, NORMAN L. Elements of Yacht Design. 1938.

PHOTOGRAPHY.

American Annual of Photography. 1941. Volume 55. 1940.

WALL, E. J. Photographic Facts and Formulas. 1940.

PHYSICS.

BURTON, E. F., H. GRAYSON SMITH, AND J. O. WILHELM. Phenomena at the Temperature of Liquid Helium. 1940.

Physical Society. Reports on Progress in Physics. Volume 6, 1940.

SANITARY ENGINEERING.

KEEFER, C. E. Sewage-Treatment Works. First Edition. 1940.

SCIENTIFIC ESSAYS.

COMPTON, ARTHUR H. The Human Meaning of Science. 1940.

NOTES FROM THE BARTOL RESEARCH FOUNDATION.

DIRECT EVIDENCE OF A PROTON COMPONENT OF THE COSMIC RADIATION.*

BY

T. H. JOHNSON, J. G. BARRY AND R. P. SHUTT.

A number of investigations [1] have resulted in more or less indirect evidence that a part of the cosmic radiation consists of protons. In a series of photographs in a large Wilson cloud chamber containing three lead plates we have obtained a few tracks which seem to be those of protons near the end of their range. The track most definitely that of a proton is shown in Fig. 1. This ray had come into the chamber from the top after having passed through fifteen centimeters of lead

FIG. 1.

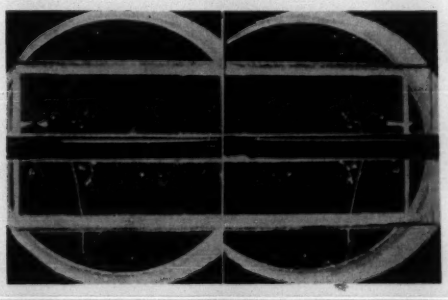

This may be viewed stereoscopically by placing a mirror before the right eye at an angle such that the image of the right projection is superposed upon the left projection when viewed directly with the left eye.

* Reprinted from *The Physical Review*, **57**, 1047 (1940).

[1] T. H. Johnson, Rev. Mod. Phys. **11**, 208 (1939); T. H. Johnson and J. G. Barry, Phys. Rev., **56** 219 (1939); D. Hughes, Phys. Rev. **57**, 592 (1940); J. G. Wilson, Proc. Roy. Soc. **172**, 517 (1939).

placed between two coincidence counters used for triggering the expansion of the chamber. In the chamber the ray has passed through three lead plates 1 cm., 5 cm., and 1 cm. thick, respectively, and it has passed out through the bottom of the chamber after having veered slightly into the shadow in the lower compartment. In the 5-cm. lead block the ray was deflected about 25° and it was slowed down so that its track in the third compartment is noticeably heavier than previously. It is significant that although its density in the third compartment seems to be about four times greater than that of a fast particle, the ray still had sufficient energy to pass through the lower plate, 1 cm. thick, and upon emerging to produce the smooth, heavy, straight track characteristic of a slow proton. In the first compartment shown enlarged in Fig. 2 the ray produced two delta-rays, or slow electrons,

FIG. 2.

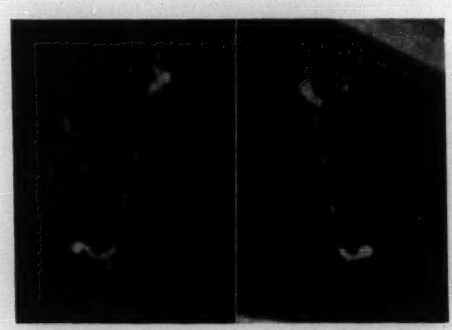

Enlargement of the track in the first compartment.

the second of which produced a track about 17 mm. long in 1.3 atmospheres of argon. From its range we estimate that this ray had an initial energy of about 55,000 volts. A ray of this energy would be emitted by a particle of infinite momentum at 77.5°. Our best estimates of its initial direction as determined from a graphical analysis of the two stereoscopic photographs lie somewhat below this angle in the range 65° to 75°.

We may consider four possibilities as to the nature of this ray. (1) The entering ray is a meson which loses energy by ionization as described by the Bethe-Heitler formula [2] and is brought nearly to rest in the lower compartment. (2) The entering ray is a proton which also loses energy by normal ionization and is brought nearly to rest in the lower compartment. (3) The entering ray is a meson which knocks a proton from a lead nucleus at an angle of 25° by an elastic collision. The subsequent path of the meson would then lie within the lead plate and the proton is that which appears in the lower compartments. (4) The entering ray is a proton with high energy (ionization less than 1.2 that of a "fast" particle) and more energy is lost in the 5-cm. lead plate than can be accounted for by ionization. For each of these assumptions the lower limit of the energy in each compartment and the corresponding upper limits of the ionization have been computed, and are given in Table I. The table also contains the angle

TABLE I.

Lower Limit of the Energy in Each Compartment and Upper Limits of the Ionization Computed Upon Various Hypotheses.

Hypothesis.	Energy of the Ray (Mev.) in Compartment.			Ionization Compared to that of a Fast Particle in Compartment.			Angle of Delta-Ray of 55,000 Volts.
	1	2	3	1	2	3	
(1) Meson	120	106	33	1.0	1.1	1.66	75.8°
(2) Proton	280	256	87	1.7	2.0	4.0	69.5°
(3) Meson-proton	480	465	87	1.0	1.0	4.0	77.3°
(4) Proton-abnormal energy loss	666	653	87	1.2	1.3	4.0	74.2°

of the delta-ray in the first compartment computed from each assumption.

From the density of the track in the third compartment it seems certain that the ray appearing in the lower half of the chamber must be a proton. The ionization in the upper half is not as heavy as would have been expected on assumption (2) and although the measured angle of the delta-ray favors

[2] S. H. Neddermeyer and C. D. Anderson, Rev. Mod. Phys. 11, 191 (1939).

assumption (4) the accuracy of the measurement is hardly sufficient to distinguish against assumption (3).

Out of 4,000 photographs we have obtained three tracks of slow protons identified by an abnormally dense ionization while the ray had still sufficient energy to penetrate 1 cm. of lead. Nineteen tracks have been found of particles either stopped or appreciably slowed down by the lead in the chamber, and in each of these photographs the observed ray had passed through the 15 cm. of lead above the chamber. It therefore appears that some fifteen per cent. of the penetrating rays reaching the "slow" state are protons. Since the range of a proton is ten times that of a meson of the same velocity about 1.5 per cent. of the fast cosmic rays can be protons.

Acknowledgment is made of the support given these studies by the Carnegie Institution of Washington.

FURTHER EVIDENCE FOR THE EXISTENCE OF MESOTRON SHOWERS.*

BY

W. F. G. SWANN and W. E. RAMSEY.

The data here recorded were obtained by an apparatus [1] which we have devised for cosmic-ray shower measurements, and which comprises several Geiger counter areas, each 20 cm. in side, arranged as a coincidence set as regards the individual areas, and designed so that each individual counter which becomes excited within 10^{-4} sec. of an event, records separately, the event being the passage through the apparatus of a ray which penetrates more than 18 cm. of lead. One tray was above the 18-cm. block, and the others were distributed at different distances below.

With the foregoing apparatus the theory of knock-on electron showers has been investigated experimentally.[1] Certain of the shower rays, a very small number, in fact, are

* Reprinted from *The Physical Review*, **57**, 1051 (1940).

[1] W. F. G. Swann, Rev. Mod. Phys. **11**, 242 (1939).

apparently of mesotron type in that they pass through several individual 1-cm. blocks of lead without multiplication, and evidence of the existence of such rays was presented at the cosmic-ray symposium held at Chicago last summer.[1] These results, which we believe to constitute the first direct evidence of the existence of mesotron pairs, have now been extended by further observations, and the results are here recorded partly in the form of a table. Table I refers in each

TABLE I.

Frequency of Two-ray Mesotron Showers.

Nature.			No.	Events.	2-Ray Mesotron Showers per 10^4 Events.
Trays.	Recorded.	Blocks.			
4	4	3	2	2300	20
4	3	3	1	2300	7
5	3	4	1	550	20

case to a situation where one ray entered the 18-cm. block of lead, and resulted in a pair of rays recording in the counter tray areas below the lead in the manner indicated in the table, which will be understood from the following scheme of designation: Under the heading *Nature*, the column *Trays* indicates the number of analyzing counter trays below the 18-cm. block. The column *Recorded* indicates the number of trays in which two rays recorded. The column *Blocks* indicates the number of individual 1-cm. blocks of lead, below the 18-cm. block, through which the pair passed and recorded subsequently *without multiplication*. The column *Number* indicates the number of cases of the kind observed in the number of events shown in the *Events*. If the numbers in the column headed *Number* were large, each case would provide a basis to allow for counter inefficiency through utilization of the numbers under the *Trays* column, and so to calculate the number of two-ray showers to be expected in 10,000 events. Such calculations, when made from the few events recorded, are given in the last column. Naturally they show wide statistical fluctuations, but serve to give an order of magnitude of 16 mesotron pairs per 10,000 events.

In addition, in the data recorded last summer, 555 events gave one case of a single ray entering the 18-cm. block and emerging as 4 which passed through one 1-cm. block without multiplication. Five hundred and seventy events gave 3 cases in which 2 rays entered the thick lead block and continued as a pair through an additional 1 cm. of lead. Five hundred and fifty-five events gave 2 cases where two rays entering the thick block emerged therefrom and passed as 2 rays through 4 individual 1-cm. blocks of lead. In the recent observations, 2,300 events gave 7 cases where two rays entering the thick block passed in addition through three individual lead blocks without multiplication or reduction.

Last summer we recorded several cases where an event was accompanied by an excitation of nearly all the counters above and all the counters below the thick block of lead. In our most recent experiments we observed nine cases out of 2,300 events where the event concerned was associated with the excitation of more than 10 counters in the tray above the thick lead block and with a perpetuation of the excitation to the counters below the lead block with no more reduction than would be expected from counter inefficiency, and without evidence of multiplication, although in such cases multiplication is difficult to rule out. It may be added that all of these experiments were performed below a 30-ft. column of water.

NOTES FROM THE BIOCHEMICAL RESEARCH FOUNDATION.

Attempts to Analyze for *d*(−) Glutamic Acid in Tissue Hydrolysates.—GLADYS E. WOODWARD AND LOUIS D. SMITH. The claim that malignant tissue proteins are made up of partially racemized amino acids, while normal tissue proteins contain only the "natural" *l*-stereoisomers, was made by Kögl and Erxleben (*Z. physiol. Chem.*, **258**, 57 (1939)) in 1939. Their claim was based on the observed optical activity of samples of the amino acids isolated from tissue hydrolysates. The difference in the case of glutamic acid was most striking. Realizing that the isolation of glutamic acid by the procedures used by Kögl and Erxleben was by no means complete, we have attempted to find a direct method of analyzing for the *d*(−) form in the protein hydrolysates without previous isolation.

For this purpose the oxidation of *d*(−) glutamic acid by *d*(−) glutamic acid oxidase described by Weil-Malherbe (*Biochem. J.*, **30**, 665 (1936)) was investigated. He had shown that *d*(−) glutamic acid was the only amino acid, of either the *d*- or *l*-series, which was oxidized by an aqueous extract of lipoid-free brain powder. If quantitative oxidation were possible by means of this enzyme, it was thought that perhaps the reaction could be used to estimate *d*(−) glutamic acid in protein hydrolysates.

An acetone-dried ether-extracted brain powder was prepared from gray matter of ox brain as described by Weil-Malherbe. An extract obtained from one part of the dry preparation and 10 or 15 parts of *M*/100 veronal buffer of pH 8.2 was tested in Warburg manometers at 38° for its effect on the oxygen consumption of *d*(−) glutamic acid. The reaction, if present at all, was so slight that it offered no hope for complete oxidation of the glutamic acid.

Application of the Cohen (*Biochem. J.*, **33**, 551 (1939)) analysis for glutamic acid was next tried. This analysis con-

sists of conversion of glutamic acid to succinic acid by chloramine *T* followed by estimation of succinic acid by means of succinoxidase. Since both the *d*- and *l*-forms of glutamic acid react, it was necessary to remove quantitatively the *l*-form before the *d*-form could be estimated by this procedure.

Yeast, during fermentation, has been generally assumed to attack only the "natural" *l*-forms of the amino acids. The utilization of *d*(−) and *l*(+) glutamic acid by yeast was therefore studied. Glutamic acid in a concentration of 0.3 per cent. was added to a fermenting-mixture containing 10 per cent. glucose and 5 per cent. yeast, and fermentation carried out at 38°. After the fermentation had ceased because of complete utilization of the glucose, samples were removed for testing. The concentration of glucose in the remaining mixture was brought to 5 per cent. and the fermentation continued. The supernatant liquid was removed by centrifugation from the samples to be tested, and the glutamic acid in this determined manometrically by the chloramine *T* reaction which was shown by Cohen to give one equivalent of CO_2 for each mole of glutamic acid. The data obtained are shown in the accompanying table.

TABLE I.

Utilization of Glutamic Acid by Fermenting Yeast.

Time of Incubation, hrs.	Loss of Glutamic Acid.		
	l(+) %	*d,l* %	*d*(−) %
Fleischmann's yeast.			
18	69	62	—
36	79	64	—
60	93	72	—
120	—	—	34
Brewers' yeast.			
90	40	35	27

The data indicate that there was no very selective utilization of the *l*-form. With Fleischmann's yeast the *l*-form

was used up much more rapidly than the *d*-form when each was present alone, but when the *d,l*-mixture was used there was indication that the presence of the *l*-form increased the utilization of the *d*-form. With brewers' yeast the action was much slower than with Fleischmann's yeast and there was no greater selectivity. Complete removal of *l*(+) glutamic acid by yeast, therefore, could not be obtained without considerable loss of *d*(−) glutamic acid.

The work of Gale (*Biochem. J.*, **34**, 392 (1940)) indicated that certain strains of *B. coli* produced an enzyme which was even more powerful than yeast in destroying *l*(+) glutamic acid. Since the enzyme was a decarboxylase which split CO_2 from the amino acid at pH 4.0, the reaction could be studied in the Warburg manometers. We have prepared four strains of *B. coli* and tested them for their decarboxylase activity using both *l*(+) and *d*(−) glutamic acid. None of these strains showed any decarboxylase activity, so this method also failed as a means of removing *l*(+) glutamic acid.

In the absence of a method for selective and quantitative removal of either the *d*- or *l*-form of glutamic acid from the *d,l*-mixture, the Cohen analytical method for glutamic acid could not be applied to estimation of the *d*-form.

BOOK REVIEWS.

ELECTROCHEMISTRY AND ELECTROCHEMICAL ANALYSIS, A THEORETICAL AND PRACTICAL TREATISE FOR STUDENTS AND ANALYSTS, by Henry J. S. Sand. Volume I, Electrochemical Theory. 133 pages, illustrations, 13 × 19 cms. Price 4 s. 6 d. Volume II, Gravimetric Electrolytic Analysis and Electrolytic Marsh Tests. 149 pages, illustrations, 13 × 19 cms. Price 5 s. London, Blackie & Son Limited.

The application of somewhat unfamiliar physical concepts to chemical analysis is always done with mistrust. It is the aim of the author of these two little volumes to dispel this condition by giving a detailed theoretical discussion with acceptable deductions followed by a description of methods. This is exactly the division of the volumes. Volume I deals with the ionic theory, conduction of the current in the interior of the electrolyte, applications of the law of mass action to the ionic theory, electromotive force and heat of reaction, theories of interionic attraction, electrode potentials—liquid junction potentials, and irreversible electrolytic processes. This coverage is direct and rigorous with little space devoted to color or background.

In Volume II attention is directed to the methods for separating metals by control of the cathode-potential with the aid of an auxiliary electrode, this given in the general treatment of gravimetric electrolytic analysis including internal electrolytic analysis, micro-chemical analysis and electrolytic Marsh tests. The size of the volumes preclude exhaustiveness of treatment but references to more specialized treatises and to original papers are made. A perusal of these volumes by those who may be interested in applying this method of analysis will be beneficial.

R. H. OPPERMANN.

TECHNICAL DRAWING, by Frederick E. Giesecke, Alva Mitchell and Henry Cecil Spencer. Second Edition, 687 pages, illustrations, plates, 16 × 24 cms. New York, The Macmillan Company, 1940. Price $3.00.

The advance of the engineering sciences has made taboo the old and only requirements of applicants for positions as draftsmen that they state they are qualified and show a sample of lettering. While skill in drawing still plays a large part, technical drawing has become highly specialized with the particular branch of the engineering sciences to which it applies. To become a finished draftsman requires a knowledge of the details of construction employed in the particular branch of engineering.

This book has for its purpose a comprehensive treatment of the science of technical drawing arranged logically, and containing a large group of practical problems. It is in its second edition, having been increased in scope to meet varied needs. In the beginning there is given a description of the instruments and materials and an explanation of their use. The geometry of technical drawing involves the solution of many practical problems which are given followed by pro-

jections, multi-view projection, auxiliary views, revolutions and sectional views. A chapter on axonometric projection includes separate divisions on isometric drawing and dimetric drawing. Oblique projection comes next before perspective, and intersections and developments. There are also special chapters on dimensioning, representation of fasteners, shop processes, working drawings, gearing and cams, pipes and fittings, welding representation and technical sketching. There are twenty-nine chapters to the book containing a fund of information some of which is unusual in a book of this type and useful on special occasions. An example is the rules for patent office drawing contained herein.

Because of the completeness of coverage and the wide scope of the book it may be used to advantage as a drawing text, in whole or in part, in collaboration with a course in engineering. There is an appendix containing much information in the way of signs and symbols and the drawing room standards of the American Standards Association. This, together with a very comprehensive subject index makes the book valuable also as a work for reference.

R. H. OPPERMANN.

FUNDAMENTALS OF PHOTOGRAPHY, WITH LABORATORY EXPERIMENTS, by Paul E. Boucher. 304 pages, plates, illustrations, tables, 16 × 24 cms. New York, D. Van Nostrand Company, Inc., 1940. Price $3.00.

Photography as a hobby may be practiced for many specific purposes by merely taking pictures. At one time or another there is likely to appear a good picture among the large number taken, although neither technique nor art is applied. But few practice this sort of photography very long, for the urge is strong to master those things necessary to correctly anticipate a good picture. It has only been of quite recent time that books such as the one at hand have been available that cover the subject in its modern light.

This book is of the type of a text, each chapter ending with a series of questions for exercise. It is of a grade suitable for college work, requiring high school training in mathematics, physics, and chemistry for a basis to obtain the most from it. The style of presentation, however, is of the kind that facilitates study and this is so to the extent that the use of the book is not restricted to the classroom but can be profitably used by anyone, individually, without benefit of instruction. Thus, an average hobbyist may follow it to advantage, if his interest is sufficiently aroused.

There are some three hundred pages to the book excluding appendixes containing useful tables, formulary and glossary. This alone tends to testify as to completeness of coverage. About two hundred and fifty pages are devoted to straight text divided into sixteen topics. These include descriptive and explanatory matter on developers and fixing solutions, lenses and diaphrams, camera shutters, photographic filters and films, enlarging, intensification and reduction, toning and dye staining prints, and color photography. The remaining pages are devoted to descriptions of seventeen laboratory experiments, helpful and extremely interesting. These experiments are covered in some detail and offer an unusual aid in following the text. At the same time a certain amount of experience is acquired.

At the end of the book there is a subject index for reference purposes. As a text in a prescribed course the book fulfills its purpose and should be examined by

teachers of the subject. For the amateur there is this to be said: Practice and theory are closely interwoven. Information given is confined to a limited space although not to a detrimental extent. Assumption is made of a high school grade of knowledge in certain subjects. Technique is stressed more than art. And lastly, because of the state of the subject, some of the aspects are of necessity controversial. With these in mind, the book can be recommended to the serious minded amateur with patience, who desires a thorough grounding in fundamentals.

R. H. OPPERMANN.

INTRODUCTION TO ELECTRICITY AND OPTICS, by Nathaniel H. Frank. First Edition, 397 pages, illustrations, 17 × 24 cms. New York, McGraw-Hill Book Company, Inc., 1940. Price $3.50.

This text is designed primarily to fit into a special place in a course of instruction. The author states it is directed toward the furnishing of a foundation for students of electrical engineering or physics at Massachusetts Institute of Technology in their second year. The book, however, being a text on fundamentals should draw the attention of workers in this field as well as teachers because it may contain an approach from a different direction and thus reveal information in a new light that has lasting significance.

Beginning with a study of the nature of electrostatic fields of force it proceeds to a detailed discussion of the production of electrostatic fields, inquiring into the laws which govern the dependence of such fields on the positions and magnitudes of the charges which produce them. The topics of induced charges and capacity, and steady electric currents precede what may be used as an illustration of unusual presentation. This is in the treatment of magnetism. Here the customary historical or narrative type of treatment of magnetism utilizing permanent magnets as the basis is discarded to avoid confusion often resulting from drawing the usual analogies between magnetic and electrostatic phenomena. Discussion of permanent magnets is delayed and the start is made from the results of the experiments of Ampere to develop the idea of a magnetic field and the forces which these fields exert on conductors carrying steady currents and on moving charges.

The coverage of induced electromotive forces and inductance leads to the subject of elementary alternating current circuits and displacement current and electromagnetic waves, the latter including an introduction to the concept of the Maxwell displacement current, a discussion of electromagnetic waves in free space, and the Poynting vector. This concludes the first half of the book.

The second half encompasses the electric and magnetic properties of matter and is based essentially on the electron theory of matter. This begins with the study of radiation of electromagnetic waves, electronic conduction in vacuum and in metals, and dielectrics. It then proceeds to show that the laws of reflection and refraction of electromagnetic waves at dielectric boundaries are derived from the electromagnetic boundary conditions and the problem of intensity relations for normal incidence is discussed in detail. An elementary theory of the dispersion and scattering of light in gases is extended to give a physical picture of the nature of the refracted wave in isotropic and anisotropic media, the latter leading to the phenomena of double refraction. The concluding chapters are on interference and diffraction, and heat radiation.

The order of presentation throughout is in accordance with the principle of introducing basic concepts one at a time wherever practical. There is a logical sequence and smooth passage. This text is worth an examination by all who may be interested in the subject.

R. H. OPPERMANN.

ELECTRICAL TIMEKEEPING, by F. Hope-Jones. 275 pages, illustrations, plates, 15 × 23 cms. London, N. A. G. Press Ltd. Price 10 s.

While this is a second edition of Electric Clocks 1931 by the same author, the historical chapters have been condensed and chapters added containing new material so that the book can reasonably be called a new work rather than a new edition.

The historical chapters record the stages of development of electrically driven pendulums from the time of Alexander Bain's patent of 1840 to the free pendulum clock resulting from the collaboration of Messrs. Hope-Jones and Shortt. During this period of approximately a century there were over one thousand patents, most of which are useless, due to either the ignorance of the inventors of each other's work or to the violation of the principle that a pendulum must have the least interference possible and yet be kept oscillating at a constant amplitude. Many mechanical and electromechanical devices are illustrated and sufficiently discussed to show the "blind alley" or the unexpected virtue that was perhaps not appreciated by the inventor himself, but that became useful at a latter date.

The Shortt clock had been installed in the observatory at Greenwich for only five years when "Electric Clocks" was written, but with this edition fifteen years' experience has accumulated. Thus there are data showing the effect of the nutation of the earth upon the rate of a clock which demands an accuracy of the order of a few thousandths of a second, and also data showing the effect of the variation in gravity due to the moon upon the rate of a clock which requires an accuracy of the order of ten thousandths of a second. Data are given of a Shortt clock that ran a year so close to the mean rate of 0.0019 second per day that its accumulated error was only 0.7 second at December 31st, which represents an accuracy of one part in 30 million. Another instance is given (SH 44 installed in the Paris observatory), of a clock having an accumulated error for the year of 1927 of 0.1 second suggesting an accuracy of one part in 300 million.

The author discusses means of popularizing the free pendulum and has devised an ingenious arrangement where the master and the slave pendulums are contained in one case, the former being the usual seconds pendulum while the latter beats half seconds. The synchronizing control between the master and the slave pendulum is mechanical. The use of a half second pendulum leads to a discussion of synchronization by circular error which is particularly applicable to a half second pendulum although generally unsatisfactory for a second pendulum.

Three chapters are allotted to the use of alternating current in time-keeping, one discussing the National Time Service provided by the "Grid" and describes clocks used for frequency checking, another discussing synchronous motor clocks, and the third describing synchronization from the A.C. supply. The last chapter is devoted to the subject of timekeeping at sea.

The book is not only of interest to horologists and electricians, but to a far wider circle since it describes the life work of one who has been completely interested in securing perfection in time-keeping and who has had a high degree of success in attaining his ambition.

B. J. WILSON.

STRENGTH OF MATERIALS, PART I, ELEMENTARY THEORY AND PROBLEMS, by S. Timoshenko. Second Edition, 359 pages, illustrations, 16 × 23 cms. New York, D. Van Nostrand Company, Inc. Price $3.50.

This well-known test first published in 1930 now appears in its second edition. The division into two parts is still retained; the book at hand being the second edition of the first part will be followed later by the second edition of part two. Those who are familiar with the first edition will find here a more modern book in point of view of clarity to the end of facilitating understanding.

Part one covers the more elementary aspects of the subject. It consists of ten chapters covering tension and compression within the elastic limit analysis of stress and strain shearing force and bending moment stresses in transversally loaded beams, deflection of transversally loaded beams, statically indeterminate problems in bending, beams of variable cross section, combined bending and tension or compression, torsion and combined bending and torsion, and energy of strain.

A feature of the treatment is that the method of presentation narrows the gap that exists between theory and practice. Evidence of this, in addition to appearing throughout the text, is particularly noticeable in the problems at the end of chapters. An appendix containing a treatment on moments of inertia of plain figures, an author and a subject index can be found in the back of the book. Covering about the same ground as the first edition of part one, but much improved, this book warrants the attention of teachers and students of the subject.

R. H. OPPERMANN.

SILVER IN INDUSTRY, edited by Lawrence Addicks. 636 pages, illustrations, tables, 16 × 24 cms. New York, Reinhold Publishing Corporation, 1940. Price $10.00.

The opening chapter of this book explains some of the history and economic background of silver. Since the first silver was taken from the ground something of the order of eighteen billion ounces has been recovered. Speaking in very round numbers, one third of this amount is today in monetary stocks, including bullion reserves; one third is in hoards, including useful articles; one third has been mislaid in unknown caches or wasted through use, carelessness or mishap. Many factors have bearing on the market for and price of silver. The value of silver in terms of gold has varied through the centuries, but until modern times a long range average of about 13 to 1 has been maintained while local departures from the rule have generally been downward. Today's commercial ratio is about 100 to 1. Total collapse of the market has been avoided solely by the buying operations of the United States Treasury. Industrial consumption is the only refuge, and the ultimate issue may well depend upon what extent and how quickly the industrial uses for silver can be developed. This book is dedicated to furthering the industrial application of silver by recording what has already been accomplished and pointing out likely lines of advance.

The treatment proper opens with a discussion of the properties of silver which is virtually a revision of the National Bureau of Standards Circular C–412. The author is A. J. Dornblatt of the Bureau. He further discusses binary silver alloys wherein base metal alloys may be improved by the addition of silver, of which, outside of the patent literature, there is little information. A summary of data on ternary silver alloys and non-ferrous engineering alloys such as brasses, bronzes, and light alloys to which a small percentage of silver was added is given by Mr. Dornblatt and A. M. Setapen which is followed by a discussion on the mechanical properties of silver and matters pertinent to its commercial production in usuable form.

One of the valuable qualities of silver which may lead to further applications in industry is the ease with which it may be welded or bonded at only slightly elevated temperatures, or even at room temperature under proper conditions. In some uses of silver this behavior may operate as a disadvantage in causing sticking of silver surfaces in contact. In addition to a discussion of the cold bonding properties, there is given some quantitative data thereon obtained in the metallurgical laboratory at Lehigh University by Allison Butts, G. R. Van Duzee, and J. M. Thomas. Subsequent chapters in the book by different authors include high temperature bonding, the use of silver in bearings, coatings, electrical contacts, silver as a catalyst, the oligodynamic effect of silver, and silver as a fungicide. A brief summary of the entire book is given in the back by Lawrence Addicks. Here the technical field is divided into four groups. The metallurgical division is held to have the greatest hopes for large new consumption. Photography is the outstanding chemical use of silver but much of its importance is cancelled by ultimate scrap recovery. The field of silver bearing electrical contacts is rapidly growing, while the consumption possibilities in the inviting field of biology are quite unknown.

The case for silver is adequately presented in this book. It is the result of an exhaustive examination of a fund of material coupled with a thorough knowledge of the subject. A very large bibliography including patents is appended together with a comprehensive subject index. A group of the principal American silver producers gave very generous support and the National Bureau of Standards and several of the eastern universities have cooperated in making the work available. The information it contains and its manner of presentation should arouse interest and be of assistance to those who have problems to solve where silver might be used.

R. H. OPPERMANN.

PUBLICATIONS RECEIVED.

The Dozen System, an Easier Method of Arithmetic, by George S. Terry. 55 pages, illustrations, 24 × 29 cms. Longmans Green and Co., New York, 1941. Price 50 cents.

The Ring Index, A List of Ring Systems Used in Organic Chemistry, by Austin M. Patterson and Leonard T. Capell. 661 pages, 16 × 24 cms. New York, Reinhold Publishing Corporation, 1940. Price $8.00.

Science on Parade, by A. Frederick Collins. 314 pages, illustrations, 15 × 21 cms. New York, D. Appleton-Century Company, 1940. Price $3.00.

Catalysis, Inorganic and Organic, by Sophia Berkman, Jacque C. Morrell and Gustav Egloff. 1130 pages, illustrations, tables, 16 × 24 cms. New York, Reinhold Publishing Corporation, 1940. Price $18.00.

Proceedings of the Michigan-Life Conference on New Technologies in Transportation, November 1, 2, 3, 1939. 231 pages, illustrations, 15 × 23 cms. Ann Arbor, University of Michigan.

Physical Chemistry, An Introduction, by E. A. Moelwyn-Hughes. 660 pages, illustrations, 19 × 28 cms. Cambridge, University Press, 1940. Price $9.50.

Canada, Department of Trade and Commerce, Dominion Bureau of Statistics. Annual Report on the Mineral Production of Canada, during the calendar year 1938. 295 pages, 17 × 25 cms. Ottawa, King's Printer, 1940. Price 50 cents.

CURRENT TOPICS

Don Quixote's Nightmare.—Wind power will soon feed Vermont power lines, it is stated in the *Industrial Bulletin* of Arthur D. Little, Inc., No. 162. An engineering project with strong backing and based on studies of eminent engineers and scientists, the new Smith-Putnam wind turbine uses vanes designed rather like airplane wings, with a "wing spread" approximating that of the largest modern bombing planes. The initial experimental vento-electric station has been designed to produce 1000 kilowatts. Its location on Grandpa's Knob atop a Green Mountain ridge near Rutland, was selected after elaborate meteorological investigations as one of a number of excellent sites available. It is expected to provide wind sufficiently steady for an availability factor greater than that for stored water as used in New England or at most other hydroelectric sites. By providing a series of vento-electric stations united in a power line with one or more reservoir-fed hydroelectric stations, it is expected that a markedly increased output of firm power will enhance the value of each. Many months of development by S. Morgan Smith Company, manufacturers of hydraulic turbines and water wheels, preceded the decision to commence commercial construction. They expect vento-electric stations to provide electric power competitive with the cheapest firm power now available. The project depends not only upon current research in aerodynamics and meteorology, but also upon recent engineering developments of numerous industries. The development work specifically undertaken for this project, including extensive model tests in aerodynamic laboratories, has provided an innovation beyond all previous means of generating power from the wind. The principal problem has been to provide the generating unit with accurate speed regulation despite tremendously fluctuating wind velocities. Uncontrollable gusts would raise the output from 1000 to 3000 kilowatts in less than three seconds, and seriously overload the generator. Patentable developments are claimed to overcome this problem of speed regulation, together with other problems such as ice formation, which have arisen during development studies.

R. H. O.

Formation of Fuels—A New Theory of the Origin of Gas, Oil and Coal.—Dr. E. Berl, Research Professor, Carnegie Institute of

Technology, Pittsburgh, Pa., at the recent meeting of the American Chemical Society tumbled many previous theories overboard. An abstract of Dr. Berl's statement appears in the *American Gas Association Monthly*, Vol. XXII, No. 9. This was prepared especially for the gas industry, which is one of the industries vitally concerned with the subject. New studies on the formation of fuels have proved that according to geochemical conditions, from carbohydrates oxygen-containing bituminous coals and oxygen-free gaseous, liquid, and solid hydrocarbons are formed. Artificial carbohydrate bituminous coals upon oxidation give exactly the same aromatic oxidation products as natural coals. These carbohydrate coals upon incoalification, give exactly the same gaseous, liquid, and solid distillation products as one obtains by the dry distillation of natural bituminous coals. These studies have proved furthermore that, contrary to the present belief, asphalts are not formed by the oxidation of crude oil. Asphalts are parent material of crude oil. Upon intramolecular combustion or by hydrogenation, they are transformed into crude oil. It has been found furthermore that adsorption phenomena during the formation and migration of oil play a very important role. These new experiments have proved that most of the older theories have to be replaced by newer viewpoints stating that those very important gaseous, liquid, and solid fuels are mostly formed from one class of parent materials—from carbohydrates which nature forms anew every year in the largest amount. Geophysical considerations show that hundreds of millions of years ago when plant materials containing little if any lignin were buried, the formation of carbohydrates was much greater than now.

R. H. O.

Technology is . . .—The first paragraph of the report on Technology on the Farm just issued by the U. S. Department of Agriculture makes an effort to tell what technology is and what the book is about. It is not offered as a definition but rather an an aid to understanding: "Technology," it says, "is science, art, and invention. It is tractors, combines, corn pickers. It is hybrid corn, new kinds of wheat, soybeans, kudzu and lespedeza. It is ways to feed cows, plants, and men. It is road building and rural electrification. It is contour plowing, conservation of soil, management of forests, production of wildlife. It is marketing and distribution. It is a race between insect pests and ways to kill them. Technology is in the workshop, in the laboratory, barn, grove, field, and home. It is a social and economic force that challenges thought and ability to plan, because its many sided nature combines the intricate in-

fluences of getting and spending, savings and debt, employed leisure and unemployed relief."

R. H. O.

Total Capacity of Water Wheels Installed in Water-Power Plants in the United States 1869–1917.—The Department of the Interior, through the Geological Survey, has released for distribution a five page mimeographed report giving the total capacity of water wheels in water-power plants in the United States by states for 1869, 1879, 1889, 1902, 1907, 1912, and 1917. The capacity of water wheels for these years is calculated from data in the census reports of different industries and is considered to be reasonably accurate, although the capacity of water wheels for some years is based on interpolated and extrapolated values for some of the industries. The report shows that in 1869 the total capacity of water wheels in all industries in the United States was 1,130,000 horsepower. In 1889 the capacity of water wheels in manufacturing plants was 1,225,000 horsepower, with an estimated 367,000 horsepower in electric public utility plants, making the total for the United States 1,622,000 horsepower. Electric central stations were first utilized about 1880 for generating electricity for arc and incandescent lighting. This industry developed rapidly, and by 1889 nearly 800 steam and water power plants were in operation. In 1907 the total capacity of water wheels in the United States was 3,296,000 horsepower of which about 44 per cent. was in electric public utility plants. In 1917 the total was 6,758,000 horse power with about 73 per cent. in public utility plants. On January 1, 1940 the total capacity of water wheels in the United States was 18,500,000 horsepower, of which 89 per cent. was in publicly and privately-owned electric utility plants.

R. H. O.

Last Frontier in 1940.—When the natural frontier disappeared about 1900, fewer than 17,000,000 people lived west of the Mississippi River, CARL E. TAYLOR pointed out recently in a discussion of reclamation. This was 26.6 per cent. of the population at that time. In 1940, says Taylor, who is head of the Division of Farm Population and Rural Welfare of the Bureau of Agricultural Economics, more than 40,000,000 people are living west of the Mississippi, 30.6 per cent. of the population. "We have arrived at the day when new areas of settlement depend almost altogether on some sort of reclamation," said Taylor. "Reclamation areas constitute

the last geographic frontier of this continent, and as such they are bound to be of tremendous importance."

R. H. O.

N. Y. U. College of Engineering to Offer First Course in Research Laboratory Management.—In recognition of the rapid development of industrial research, combined with its growing importance in the national defense program, the New York University College of Engineering will offer the first course in the country in research laboratory management, it was announced recently by Dean Thorndike Saville. The outline of the course has been planned in cooperation with an advisory committee of industrial research executives headed by Maurice Holland, director, Division of Engineering and Industrial Research, National Research Council who suggested the course; Dr. W. A. Gibbons, director of development, United States Rubber Company; H. W. Graham, director of Metallurgy and Research, Jones and Laughlin Steel Corporation; Lewis N. Waters, vice-president, General Foods Corporation; Dr. Franklin Cooper, Haskins Laboratories, and Robert B. Colgate, vice-president, Colgate-Palmolive-Peet Company. "It is estimated that there has been a 100 per cent. increase in the number of research laboratories established since 1937," Dean Saville said. "These facts have caused problems of management, administration, and accounting in a branch of industry which heretofore has been comparatively free of budgetary restrictions, operating policies, and administrative organization. This tremendous growth had demanded of industry that it seek men trained in administration, accounting, organization and management who have considered the problems peculiar to this new industry in the light of its unusual functions. In addition, the national government has come to realize the importance of industrial research in any war, either armed or economic, against any foreign power or against economic distress. It will certainly be one of the country's first lines of defense," the Dean said.

R. H. O.